



COPYRIGHTED BY

Chao Ma

August 2016

**AN INVERSE SCATTERING SERIES (ISS) DATA COMPREHENSIVE  
INTERNAL MULTIPLE ATTENUATION ALGORITHM  
THAT ACCOMMODATES PRIMARIES  
AND INTERNAL MULTIPLES IN THE INPUT DATA**

---

A Dissertation

Presented to

the Faculty of the Department of Physics

University of Houston

---

In Partial Fulfillment

of the Requirements for the Degree

Doctor of Philosophy

---

By

Chao Ma

August 2016

**AN INVERSE SCATTERING SERIES (ISS) DATA COMPREHENSIVE  
INTERNAL MULTIPLE ATTENUATION ALGORITHM  
THAT ACCOMMODATES PRIMARIES  
AND INTERNAL MULTIPLES IN THE INPUT DATA**

---

Chao Ma

APPROVED:

---

Dr. Arthur B. Weglein, Chairman

---

Dr. Stuart A. Hall

---

Dr. Lawrence S. Pinsky

---

Dr. Donna W. Stokes

---

Dr. Lowell Wood

---

Dr. Nizar Chemingui

---

Dean, College of Natural Sciences and Mathematics

## ACKNOWLEDGMENTS

I would like to express my sincere gratitude to my advisor Dr. Arthur B. Weglein for the continuous support of my Ph.D. study, for his patience, encouragement, and immense knowledge. Without his guidance and persistent help, this dissertation would not have been possible. I have been always admired his profound knowledge, enthusiasm in teaching, and great sense of humor. Dr. Weglein is a great teacher who teaches not only with mind, but also with heart. What I learned from him (both technically and non-technically) will continue benefiting me throughout my professional and personal life. I am greatly indebted to him. I would also like to thank Dr. Hall, Dr. Pinsky, Dr. Stokes, Dr. Wood, Dr. Chemingui for their time and serving as members of my dissertation committee.

I am grateful to all members or alumni of the Mission-Oriented Seismic Research Program (M-OSRP). Thanks to Fang Liu, Paolo Terenghi, Xu Li, Zhiqiang Wang, and Mojdeh Niazmand for their help and guidance when I just entered the program. Thanks to James D. Mayhan, Jr., Hong Liang, Wilberth Herrera, Lin Tang, Jinlong Yang, Yanglei Zou, Jing Wu, Xinglu Lin, and Qiang Fu for for sharing all the happiness and tears together for these years. Thanks to Jennifer Chin-Davis, Naomi Haynes, and Jackqueline Owens for administrative support.

I am grateful to all M-OSRP sponsors for their continuous support and encouragement. I would like to thank Clement Kostov and Fred Hugand for providing me with the internship opportunity at WesternGeco/Schlumberger to test the Inverse Scattering Series (ISS) data comprehensive internal multiple attenuation algorithm on Kuwait Oil Company well log data. I would like to thank Nizar Chemingui for providing me with two internship opportunities at Petroleum-Geo Services (PGS) to broaden my understanding, insights and experience in seismic imaging areas.

I would like to thank my late Dad, Chengpo Ma and my Mom, Changxi Li, for raising me, giving me unconditional love and teaching me the values of kindness, generosity and appreciation with their own conduct. I would like to thank my older sister, Hui Ma, for her support and taking care the family while I am not around. I would express my sincere gratitude to my wife, Wenting Liang, for her trust, patience, understanding and wholehearted support.

**AN INVERSE SCATTERING SERIES (ISS) DATA COMPREHENSIVE  
INTERNAL MULTIPLE ATTENUATION ALGORITHM  
THAT ACCOMMODATES PRIMARIES  
AND INTERNAL MULTIPLES IN THE INPUT DATA**

---

An Abstract of a Dissertation

Presented to

the Faculty of the Department of Physics

University of Houston

---

In Partial Fulfillment

of the Requirements for the Degree

Doctor of Philosophy

---

By

Chao Ma

August 2016

## ABSTRACT

This dissertation contributes to two specific topics within the general area of exploration seismology. In exploration seismology, primaries are used to locate reflectors in a process called migration. In practice a smooth and continuous velocity is generally assumed to obtain the subsurface structural images of reflectors from recorded primaries. When using a smooth velocity model, multiples in the recorded data will result in false subsurface images of reflectors where no reflectors exist, producing an erroneous and mistaken view of the subsurface. Hence multiples need to be predicted and removed from the recorded data first, before imaging primaries.

The first part of this dissertation contributes to the removal of internal multiples using the Inverse Scattering Series (ISS). The ISS internal multiple attenuator (of a given specific order), inputs the recorded primaries and internal multiples. The primaries in the input data predict internal multiples of that order from all reflectors at once with accurate time and approximate amplitude and without subsurface information. When the internal multiples in the input data enter the ISS attenuator of a given order, they (1) contribute to higher order internal multiples removal and (2) under certain circumstances can cause false or spurious events to be predicted. Terms in the internal multiple removal subseries, which are of higher order than the ISS internal multiple attenuator, have the purpose and capability of addressing a shortcoming of its lower order and less accommodating relative. The new internal multiple algorithm within this dissertation combines the original lower order attenuation algorithm with the inclusion and assist of the higher order terms, providing a

comprehensive internal multiple attenuator that can accommodate primaries and internal multiples in the input data. That new higher-order algorithm provides all the benefit of the original ISS internal multiple attenuation algorithms without its deficits and shortcomings. This dissertation contributes to identifying those higher-order terms, and examining, testing and analyzing the relevant and practical benefit provided by this higher-order algorithm.

In principle only primaries are called for to determine structure and to identify subsurface properties. However, when the collection of primaries is incomplete and less than adequate, then the predicted multiples can, at times, be used to provide an approximate image of unrecorded primaries. The latter can supplement the subsurface structural image from recorded primaries. The second part of this dissertation contributes to (1) studying the procedure of using multiples to enhance subsurface structural imaging, and (2) examining and illustrating the added-value from that procedure.

To summarize, this dissertation contributes to two important topics in exploration seismology, (1) identifying and removing multiples and (2) using multiples. This dissertation shows multiples can be used to provide an approximate image of unrecorded primaries to enhance the subsurface structural from recorded primaries. However, multiples need to be first predicted and removed from the data before imaging the recorded primaries for processing goals that seek to effectively locate and invert reflections. The removal of multiples remains a key open issue, and high priority pressing challenge. This dissertation is part of an overall strategy to use the ISS to provide further capability for internal multiple prediction and removal in extremely complicated onshore and complex offshore exploration cases.

## CONTENTS

<b>1. Introduction and background</b> . . . . .	<b>1</b>
1.1 Exploration seismology . . . . .	1
1.2 Challenges and Strategy . . . . .	7
1.3 An overview of this dissertation . . . . .	10
<b>2. Inverse Scattering Series and internal-multiple-attenuation subseries</b>	<b>11</b>
2.1 Inverse Scattering Series . . . . .	11
2.2 Development of the inverse scattering series and its subseries for seismic processing . . . . .	14
2.3 The ISS internal multiple attenuation subseries . . . . .	16
<b>3. The ISS data comprehensive internal-multiple-attenuation algorithm that accommodates primaries and internal multiples as subevents in the input data</b> . . . . .	<b>24</b>
3.1 General output from $b_3$ in a two reflector example (Zhang and Shaw, 2010) . . . . .	25
3.1.1 Example of purpose perturbation in the ISS free-surface multiple re- moval case . . . . .	28

3.1.2	Example of purposeful perturbation in the ISS internal multiple at- tenuation case . . . . .	31
3.2	General output from $b_3$ in a three or more reflector example .	36
3.3	An ISS data comprehensive internal-multiple-attenuation al- gorithm that accommodates primaries and internal multiples in the input data . . . . .	39
4.	Numerical tests of the ISS data comprehensive internal multiple at- tenuation algorithm . . . . .	43
4.1	1D normal incident case . . . . .	43
4.2	2D case . . . . .	48
5.	Use of multiples to obtain an approximate image of an unrecorded primaries to enhance the subsurface structural imaging . . . . .	52
6.	Summary . . . . .	59
	<i>References</i> . . . . .	61
	<i>Appendices</i> . . . . .	67
	A. Derivation of equation 3.20 . . . . .	68
	B. Type I and Type II equations in Inverse Scattering Series . . . . .	72

## 1. INTRODUCTION AND BACKGROUND

This chapter provides a general background and introduction for the advances and contributions that this dissertation makes to specific data processing methods/tools used in exploration seismology. An overview of this dissertation is also provided.

### 1.1 Exploration seismology

The objective of exploration seismology is to find commercially economic subsurface deposits of crude oil, natural gas and minerals. In exploration seismology, a man-made seismic source (e.g., air-guns<sup>1</sup> for offshore exploration, dynamite<sup>2</sup> or seismic vibrators<sup>3</sup> for onshore exploration) creates waves that propagate into earth. A portion of those artificially induced waves gets reflected by subsurface rock layers, travels back to the earth surface and is recorded by seismic receivers<sup>4</sup> (e.g., hydrophone in marine, geophone on land). Figure 1.1 provides a cartoon to illustrate seismic data acquisition in marine environment. The recorded seismic waves (referred to as seismic data) are processed and interpreted by geophysicists and geologists to locate commercial-sized reservoirs. Seismic data consist of many seismic traces<sup>5</sup>.

---

<sup>1</sup>A source of seismic energy used in acquisition of marine seismic data. This gun releases highly compressed air into water ([www.glossary.oilfield.slb.com](http://www.glossary.oilfield.slb.com)).

<sup>2</sup>A type of explosive used as a source for seismic energy during data acquisition ([www.glossary.oilfield.slb.com](http://www.glossary.oilfield.slb.com)).

<sup>3</sup>A seismic vibrator is a truck-mounted or buggy-mounted device that is capable of injecting low-frequency vibrations into the earth ([www.en.wikipedia.org/wiki/Seismic\\_vibrator](http://www.en.wikipedia.org/wiki/Seismic_vibrator)).

<sup>4</sup>A device that detects seismic energy in the form of ground motion or a pressure wave in fluid and transforms it to an electrical impulse ([www.glossary.oilfield.slb.com](http://www.glossary.oilfield.slb.com)).

<sup>5</sup>The seismic data recorded by one receiver due to one source, as a function of time, is called a seismic trace.

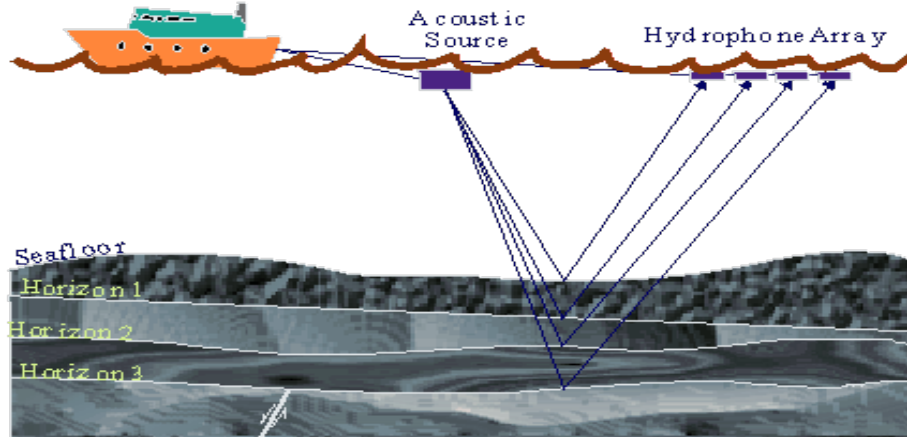


**Fig. 1.1:** A cartoon to illustrate the activity of seismic data acquisition in marine environment (<http://naturalgas.org/naturalgas/exploration/>).

Each trace contains discrete arrivals of seismic waves recorded by one receiver as a function of arrival time. Those discrete arrivals of seismic waves are referred to as “events” (see Figure 1.2).

It is useful to catalog seismic events based on their travel histories. For instance, Figure 1.3 shows different types of seismic events in marine seismic exploration. In marine seismic exploration, reference waves are *first* defined as waves that travel directly from source to receiver and waves that first travel up to the air-water boundary and then to the receiver. These two types of waves did not experience the subsurface<sup>6</sup>. All other events have experienced the subsurface. *Then*, among the waves that did experience the subsurface<sup>7</sup>, ghost events are defined as the seismic events that begin their propagation histories by traveling up from the source to the air-water boundary (source ghosts) or end their histories by traveling down from the air-water boundary to the receiver (receiver ghosts) or both (source and receiver ghosts). *After that*, events that begin their history going downward from the source and end their history upward at the receiver are divided into primary events and multiple events. Primary events are defined as the events that experience only one upward

<sup>6</sup>In the marine environment, these two types of waves are called reference wave.

<sup>7</sup>Seismic events that did experience the earth are referred to as scattered wave.

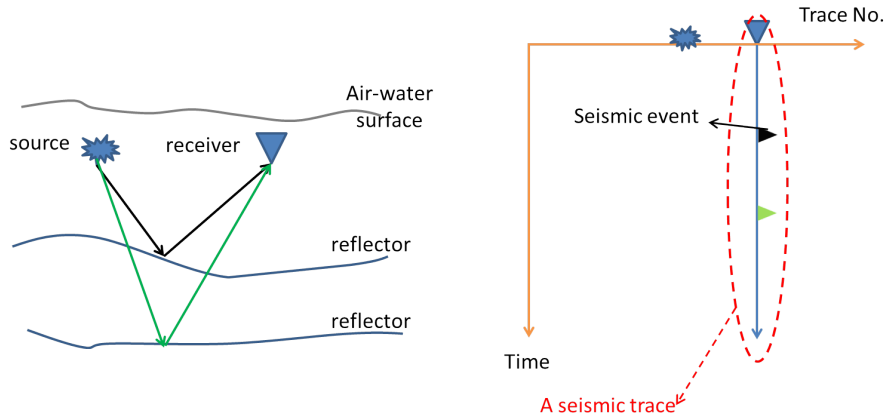


**Fig. 1.2:** The cartoon on the left shows two events with two different travel paths; the cartoon on the right shows one trace (circled by dashed red) where seismic events are represented by the black and green triangles. Seismic traces are recorded as a function of shot position ( $x_s^r$ ), receiver position ( $x_r^r$ ) and time ( $t$ ). This figure shows only one trace from one shot and one receiver. In practice, seismic data consist of many shots where each shot contains many receivers.

reflection during their propagation history, whereas multiple events are defined as the events that experience multiple reflections during their propagation history. Multiple events are further divided into free-surface multiples and internal multiples depending on the location of downward reflection between two consecutive upward reflections.

Multiples that have at least one downward reflection at the air-water (for offshore exploration) or air-land (for onshore exploration) surface are called free surface multiples, whereas multiples that have all of their downward reflections below the air-water or air-land surface are called internal multiples (Weglein *et al.*, 1997). The order of a free-surface multiple is defined as the number of reflections it has experienced only at the air-water or air-land surface. In contrast, the order of an internal multiple is defined by the total number of downward reflections below the air-water or air-land surface. Figure 1.4 illustrates of free-surface multiples and internal multiples of different orders.

Notice that, these definitions of different event types follow a sequence.

After seismic data acquisition, the next step is to find petroleum reservoirs using the sub-

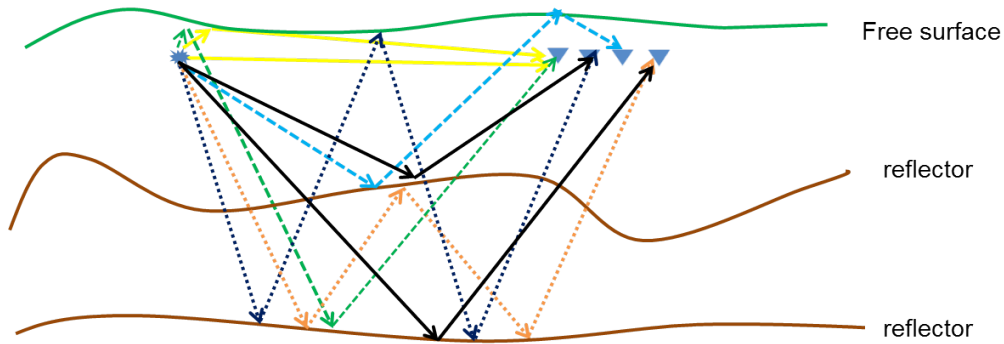


**Fig. 1.3:** Illustration of different seismic events in marine environment. Yellow solid line: reference wave; Green and light blue dashed: source ghost and receiver ghost, respectively; Dark blue dashed line: free surface multiple; Orange dashed line: internal multiple; solid black line: primary.

surface information carried by the recorded seismic data. Petroleum reservoirs are usually located in structural traps<sup>8</sup>. A structural mapping of subsurface reflectors helps to locate those traps and an estimation of properties (such as velocity, density) change across the subsurface reflectors helps to determine if crude oil or natural gas is there once those traps were located. Hence, the subsurface information that people want to get from seismic data include, e.g., where the reflectors locate in the subsurface and how the mechanical properties change across those reflectors. The process to locate the subsurface reflectors is called imaging, and the process to estimate the mechanical properties change across the reflectors is called inversion.

Different imaging methods are developed to locate the subsurface reflectors based on different imaging principles. For example, imaging methods that are used a lot today by the petroleum industry (e.g., Claerbout (1971); Whitmore (1983); Baysal *et al.* (1983); McMechan (1983)) are based on the imaging principle of space-time coincident of upgoing and downgoing waves, while the recently developed imaging method (Weglein *et al.*,

<sup>8</sup>In petroleum geology, a structural trap is a type of geological trap that forms as a result of changes in the structure of the subsurface, due to tectonic, diapiric, gravitational and compactional processes. These changes block the upward migration of hydrocarbons and can lead to the formation of a petroleum reservoir.

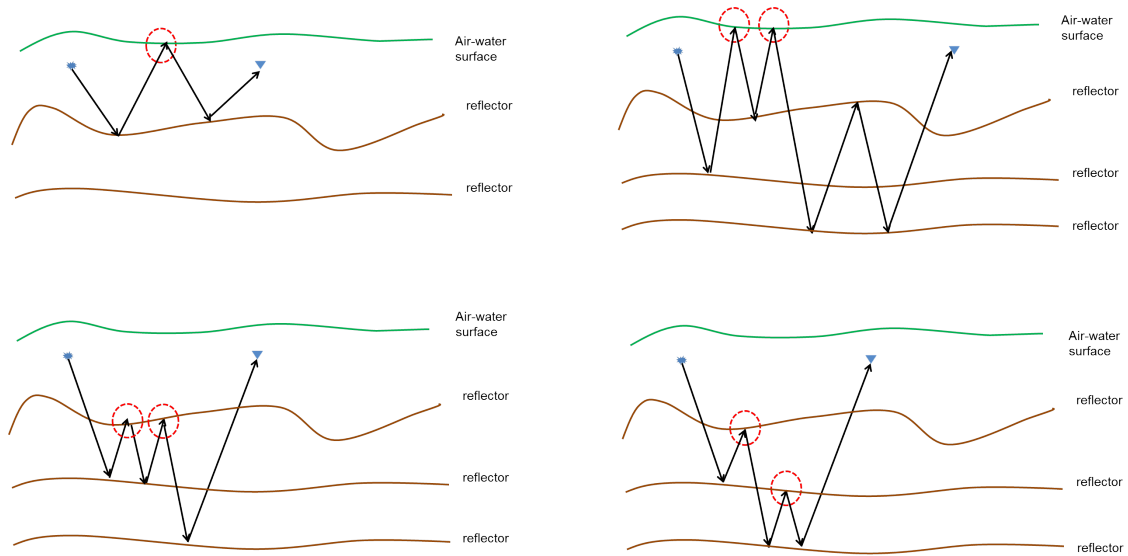


**Fig. 1.4:** The top-left, top-right, bottom-left and bottom-right cartoon are first-order free-surface multiple (one downward reflection at the air-water surface), second-order free-surface multiple (two downward reflections at the air-water surface), second-order internal multiple (no downward reflections at the air-water surface, total of two downward reflections below the air-water surface) and second-order internal multiple (no downward reflections at the air-water surface, total of two downward reflections below the air-water surface), respectively.

2011a,b; Liu and Weglein, 2014) that is well founded and physically interpretable is based on the imaging principle of coincident source-receiver experiment at depth at time equals zero. A velocity information is required as input in imaging methods based on both aforementioned imaging principles<sup>9</sup>. In practice, a smooth and continuous velocity is generally assumed. When a smooth and continuous velocity is used, only primaries are required to locate reflectors, while other events, such as multiples, result in false images of reflectors in imaging methods based on both imaging principles<sup>10</sup> (Weglein, 2016). Therefore, events except for primaries need to be removed<sup>11</sup> from the seismic data before inputting the seismic data to imaging and inversion algorithms to locate the reflectors and estimate properties change.

The removal of reference wave, ghosts and multiples are usually achieved in stages. A typical series of tasks to process the seismic data after its acquisition follows the sequence shown below:

1. reference wave removal and deghosting;
2. free-surface multiple removal;
3. internal-multiple removal;
4. seismic imaging and inversion.

Steps (1) is usually called seismic data pre-processing, while step (2), (3) and (4) are usually called seismic data processing. It should be mentioned that except for the first step whose input is recorded seismic data, the input to every other step in the sequence is the output

---

<sup>9</sup>The ISS provides an ISS imaging algorithm (e.g., Weglein *et al.* (2003); Shaw (2005)) that does not require any subsurface information, such as velocity information.

<sup>10</sup>In fact, when an accurate discontinuous velocity model is used, only primaries contribute to migration with the same image and inversion results independent of whether multiples are kept or removed (Weglein, 2016).

<sup>11</sup>However, it should be mentioned that reference wave can be utilized to estimate the source wavelet (Weglein and Secret, 1990). A wavelet is used to describe a short time series which can be used to represent, for example, the source characteristics.

from the last step. Hence, how well all the earlier steps in the flow have been achieved will affect the effectiveness of any given later step. For example, the steps to remove free-surface multiples (e.g., Carvalho *et al.* (1991); Weglein *et al.* (1997)) and internal multiples (e.g., Araujo *et al.* (1994); Weglein *et al.* (1997)) are non-linear processes in terms of input data, therefore, any errors in reference wave removal and deghosting will diminish the effectiveness in removing multiples.

After removing reference wave, ghosts, free-surface multiples and internal multiples from the data, the seismic data now contain only primary events. Then, imaging and inversion algorithms take primaries as input and output subsurface structural mapping and mechanical parameter estimation to find subsurface deposits of crude oil, natural gas and minerals<sup>12</sup>.

## 1.2 Challenges and Strategy

Multiple removal is a long-standing problem. Many methods have been developed in seismic exploration history based on the assumptions of the data characteristic or the nature of the earth (Weglein and Dragoset, 2005). These methods are often effective when the assumptions are satisfied. However, as the petroleum industry moves to ever more complex and challenging offshore and onshore plays, providing detailed and accurate subsurface information has become (and will continue to become) increasingly difficult to satisfy. The inability to adequately provide that accurate and detailed subsurface information is a contributing factor to the breakdown and failure of seismic processing methods and subsequent dry hole drilling. That drives the search for capabilities that will not require subsurface information (Weglein, 2013).

The Inverse Scattering Series (ISS) provides a procedure to achieve all processing objectives directly and without subsurface information. This procedure can be divided into a set of

---

<sup>12</sup>In addition to seismic method, other methods such as gravitational, magnetic, electrical and electromagnetic methods are also used to achieve the ultimate goal of finding subsurface deposit of resources.

steps: (1) removal of free-surface multiples; (2) removal of internal multiples; (3) imaging and (4) inversion. Each step is achieved by a subset of the inverse scattering series which is identified. For example, an ISS internal multiple removal subseries is identified and used to derive the current ISS internal multiple attenuation algorithm. This ISS internal multiple attenuation algorithm has shown differential added-value, in comparison with other internal multiple suppression methods, for complex exploration areas where internal multiple generators are difficult to be identified (e.g., Matson *et al.* (1999); Fu *et al.* (2010); Hsu *et al.* (2010); Ferreira (2011); Terenghi *et al.* (2011); Luo *et al.* (2011); Weglein *et al.* (2011); Kelamis *et al.* (2013)). It can predict internal multiples (with exact time and approximate amplitude) at all depths by combining primaries in the input data as subevents without subsurface information. This algorithm has been recognized as the most capable internal multiple suppression method by the petroleum industry. For example, at the 2013 Post-Convention Society of Exploration Geophysicists (SEG) Internal Multiple Workshop (Thursday, September 26, 2013), nine of the eleven presentations describe and exemplify the industry-wide impact and stand-alone capability (for complex offshore and onshore plays) of the ISS internal multiple attenuation algorithm.

The ISS internal multiple attenuation algorithm consists of the ISS internal multiple attenuators of different orders. Each internal multiple attenuator of given order uses primaries in the input data to predict internal multiples of that order from all reflectors at once with accurate time and approximate amplitude and without subsurface information. However, the input data consist of both primaries and internal multiples. When the internal multiples in the input data enter the ISS attenuator of a given order, they (1) contributes to higher-order internal multiple removal and (2) under certain circumstances can cause false or spurious events. Terms in the internal multiple removal subseries, which are of higher order than the ISS internal multiple attenuator, have the purpose and capability of addressing a shortcoming of its lower order and less accommodating relative. The new internal multiple algorithm within this dissertation combines the original lower order attenuation algorithm

with the inclusion and assist of the higher order terms, providing a comprehensive internal multiple attenuator that can accommodate primaries and internal multiples in the input data. That new higher-order algorithm provides all the benefit of the original ISS internal multiple attenuation algorithms without its deficits and shortcomings.

This first part of this dissertation contributes to identifying those higher-order terms, and examining, testing and analyzing the relevant and practical benefit provided by this higher-order algorithm. It is also part of an overall strategy to use the ISS to provide further capability for internal multiple prediction and removal in extremely complicated onshore and offshore exploration cases.

As described in the Abstract, in principle, only primaries are called for to determine structure and to identify subsurface properties. Multiples, along with reference wave, ghosts, need to be predicted and removed from the seismic data in order to obtain the primary-only input to the imaging and inversion methods. However, when the collection of primaries is incomplete and less than adequate, then the predicted multiples can, at times, be used to provide an approximate image of unrecorded primaries. The latter can supplement the subsurface structural image from recorded primaries. The second part of this dissertation contributes to (1) studying the procedure of using multiples to enhance subsurface structural imaging, and (2) examining and illustrating the added-value from that procedure. As pointed out in Weglein (2016), while multiples can be useful to provide an approximate image of unrecorded primaries to supplement subsurface structural imaging, it is necessary and important to point out and underline several points. (1) In practice, a smooth and continuous velocity is generally assumed and only recorded primaries are required to obtain the subsurface structural image of reflectors. Multiples need to be removed first from data before imaging the recorded primaries for processing goals that seek to effectively locate and invert reflections. The use of multiples cannot be a distraction from the high priority of developing the next level of capabilities to remove multiples to allow recorded primaries to

deliver their promise and potential. (2) If the collection of primaries is adequate, multiples are not needed to provide an approximate image. (3) The use of multiples produces a lower level and less capable form of images from the unrecorded primaries than imaging actual recorded primaries. (4) There are artifacts (e.g., cross-talks) produced in the procedure of using multiples, hence, this procedure needs to be judiciously implemented.

### 1.3 An overview of this dissertation

As described earlier, this dissertation contributes to two specific topics within the general area of exploration seismology. The first topic of this dissertation is providing a comprehensive internal multiple attenuator that can accommodate primaries and internal multiples in the input data. It is discussed from chapter 2 to chapter 4. Following Weglein *et al.* (2003), chapter 2 provides an introduction to Inverse Scattering Series and the current ISS internal multiple attenuation algorithm. Chapter 3 describes the extended ISS data comprehensive internal multiple attenuator which can accommodate primaries and internal multiples in the input data and retain the unique effectiveness of current algorithm. Chapter 4 provides numerical examples to demonstrate the added-value this extended data comprehensive algorithm can provide in complex offshore and onshore exploration seismology plays. The second topic of this dissertation is studying the use of multiples to provide an approximate image of unrecorded primaries and examining and illustrating the added-value from that procedure. It is discussed in chapter 5. Chapter 6 provides a summary of this dissertation.

## 2. INVERSE SCATTERING SERIES AND INTERNAL-MULTIPLE-ATTENUATION SUBSERIES

This chapter provides an introduction on Inverse Scattering Series, its development on different subseries on different seismic data processing tasks. Understanding the theory background of ISS methods will help us understand why this powerful algorithm can achieve all the seismic processing objectives in principle without needing any subsurface information.

### 2.1 Inverse Scattering Series

Scattering theory is a form of perturbation analysis, it describes how a perturbation in the properties of a medium relates a perturbation to a wavefield that experiences that perturbed medium (Weglein *et al.*, 2003). It is customary to consider the unperturbed medium as the reference medium. The difference between the actual and reference media is characterized by the perturbation operator. The corresponding difference between the actual wavefield and reference wavefield is called the scattered wavefield. Forward scattering takes the reference medium, the reference wavefield and perturbation operator as input and outputs the actual wavefield. Inverse scattering takes the reference medium, the reference wavefield and values of the actual field on the measurement surface as input and outputs the difference between actual and reference medium properties.

Following Weglein *et al.* (2003), I start the mathematical description of scattering theory

with the differential equations governing wave propagation in the media.

$$LG = \delta(\vec{r} - \vec{r}_s) \quad (2.1)$$

$$L_0G_0 = \delta(\vec{r} - \vec{r}_s) \quad (2.2)$$

where  $L$ ,  $L_0$  are differential operators in the actual and reference medium, respectively.  $G$ ,  $G_0$  are actual and reference wavefield, respectively.  $\vec{r}$ ,  $\vec{r}_s$  are receiver and source location, respectively. Define the perturbation as  $V \equiv L_0 - L$ .

Notice that the differential operator  $L$  and  $L_0$  represents the properties of the actual and the reference medium; different earth model-types are described by different form of operators.

We can express the actual medium in terms of a reference medium and a perturbation as  $L = L_0 - V$ . Thus, equation 2.1 can be written as

$$(L_0 - V)G = \delta, \quad (2.3)$$

$$L_0G = \delta + VG, \quad (2.4)$$

With the solution of  $G_0$  from  $L_0G_0 = \delta$  (i.e., equation 2.2),  $G$  can be solved as follows<sup>1</sup>,

$$G = \int G_0(\delta + VG) = G_0 + G_0VG. \quad (2.5)$$

The last equation is called Lippmann-Schwinger equation (e.g., Taylor (1972)), which is essentially an integral equation.

---

<sup>1</sup>If  $G$  and  $G_0$  satisfy equations  $LG = -\delta(\vec{r} - \vec{r}_s)$  and  $L_0G_0 = -\delta(\vec{r} - \vec{r}_s)$ , then  $V$  is defined as  $V \equiv L - L_0$ . But the Lippmann-Schwinger equation stays the same.

Iteratively substituting equation 2.5 into itself gives the forward scattering series,

$$\begin{aligned}\psi_s &= G_0 V G_0 + G_0 V G_0 V G_0 + G_0 V G_0 V G_0 V G_0 + \dots \\ &= (\psi_s)_1 + (\psi_s)_2 + (\psi_s)_3 + \dots\end{aligned}\tag{2.6}$$

where  $\psi_s = G - G_0$  is the scattered wavefield, and  $(\psi_s)_n$  is the portion of  $\psi_s$  that is  $n^{th}$  order in  $V$ . The data  $D$  is the scattered wavefield evaluated on the measurement surface  $D = (\psi_s)_{ms}$ .

Equation 2.6 can be used as a modeling tool to obtain seismic wavefield on the measurement surface  $(\psi_s)_{ms}$ , given reference wavefield  $G_0$ , and perturbation  $V$  (the difference between the reference and actual medium properties).<sup>2</sup>

To derive the inverse scattering series, expanding the perturbation  $V$  as a series

$$V = V_1 + V_2 + V_3 + \dots,\tag{2.7}$$

where  $V_n$  is the portion of  $V$  that is  $n^{th}$  order in the data,  $D$ . Substituting equation 2.7 into equation 2.6 and evaluating both sides on the measurement surface and setting terms of equal order in the data equal gives the following set of equations

$$(\Psi_s)_m = (G_0 V_1 G_0)_m,\tag{2.8}$$

$$0 = (G_0 V_2 G_0)_m + (G_0 V_1 G_0 V_1 G_0)_m,\tag{2.9}$$

$$0 = (G_0 V_3 G_0)_m + (G_0 V_2 G_0 V_1 G_0)_m + (G_0 V_1 G_0 V_2 G_0)_m + (G_0 V_1 G_0 V_1 G_0 V_1 G_0)_m,\tag{2.10}$$

$$0 = (G_0 V_n G_0)_m + (G_0 V_1 G_0 V_{n-1} G_0)_m + \dots + (G_0 V_1 G_0 V_1 G_0 V_1 \dots G_0 V_1 G_0)_m.\tag{2.11}$$

$V_1$  can be solved in equation 2.8 using the measured scattered wavefield  $(\psi_s)_m$  and the

---

<sup>2</sup>Matson (1997) provides analytic examples to use equation 2.6 to obtain wavefield.

reference wavefield  $G_0$ . Then, substitute  $V_1$  into equation 2.9, solve for  $V_2$  as in equation 2.8. In this manner, we can compute any  $V_n$  only using the measured scattered wavefield  $(\psi_s)_m$  and the reference wavefield  $G_0$ . Hence  $V = \sum_{n=1}^{\infty} V_n$  is an explicit direct inversion framework.

## 2.2 Development of the inverse scattering series and its subseries for seismic processing

The inverse scattering series methods were first developed by Moses (1956); Prosser (1969) and Razavy (1975). Weglein *et al.* (1981) and Stolt and Jacobs (1980) applied the inverse scattering series methods to extract multidimensional earth information from seismic data. The inverse scattering series provides a direct method to determine the physical properties of the subsurface using only measured data and reference medium. The important pioneering work on convergence criteria for the inverse scattering series by Prosser (1969) provides a condition which is difficult to translate into a statement on the size and duration of the contrast between actual and reference media. Carvalho (1992) performed empirical tests for a 1D acoustic medium without any subsurface information. The result indicated the full series only convergences when the difference between the actual earth's acoustic velocity and reference velocity (water velocity) is less than 11%.

An apparent lack of robust convergence<sup>3</sup> of the overall series suggested by numerical tests motivates the concept that inversion can be viewed as a set of steps where each step is achieved by different, task-specific subseries corresponding to that specific task. For example, each step in inversion can be defined as achieving a task or objective: (1) removing free-surface multiples; (2) removing internal multiples; (3) locating and imaging reflectors in space; and (4) determining the changes in earth material properties across those reflectors.

---

<sup>3</sup>There are other factors that motivate the idea of developing distinct and task-specific subseries. See Weglein *et al.* (2003) for more details.

The idea was to identify, within the overall series, specific distinct subseries that performed these focused tasks and to evaluate these subseries for convergence, requirements for a priori information, rate of convergence, data requirements and theoretical and practical prerequisites. It was imagined (and hoped) that perhaps a subseries for one specific task would have a more favorable attitude towards, e.g., convergence in comparison to the entire series.

As mentioned in Weglein *et al.* (2003), the pursuit of task-specific subseries used several different types of analysis with testing of new concepts to evaluate, refine and develop embryonic thinking largely based on analogues and physical intuition. For example, for internal multiples, understanding how the forward scattering series produces an internal multiple event provides a “hint” where the inverse process might be located. That “hint”, due to a symmetry between event creation and event processing for inversion, turns out to be a suggestion, with an infinite number of possible realizations. Intuition, testing and subtle refinement of concepts ultimately pointed to where the inverse process was located. Once the location was identified, further rationalizations could be provided to explain the choice among the plethora of possibilities.

Once the subseries was located, another issue that these task-specific subseries faced was how many terms would be required in practice to achieve a certain level of effectiveness towards the specific task associated with that subseries. The concept of purposeful perturbation was developed to address this issue (Weglein *et al.*, 2003). The idea is to identify the specific purpose or role that each term within a task-specific subseries performs independent of the subsurface or target over which the recorded data were collected<sup>4</sup>. For example, in the ISS internal multiple attenuation subseries (Araújo, 1994; Araujo *et al.*, 1994; Weglein *et al.*, 1997), the task of each term was understood to attenuate a given order of internal multiples in the data; this task is accomplished regardless of the convergence of the series. Hence, a thorough understanding of what task can be achieved by each term in a specific subseries

---

<sup>4</sup>The specific role that each term plays within a task-specific subseries was understood during the locating and identifying each term in the inverse process.

provides a guidance for its practical use and it mitigates the concern of overall convergence. In addition, a knowledge of the role that each term plays in a specific subseries extends our understanding of the series and provides a guidance for selecting additional terms for more ambitious inversion objectives and capability.

### 2.3 The ISS internal multiple attenuation subseries

Distinct subseries can be isolated from the overall series to achieve different tasks. The development of the specific subseries to remove internal multiples from ISS uses the analogy between the forward and inverse series (Weglein *et al.*, 1997, 2003). It was shown in Matson and Weglein (1996) that the forward series could generate primaries and internal multiples through the action of  $G_0^d$  in  $V$ , where  $G_0^d$  is a whole space Green's function and  $V$  is the perturbation operator<sup>5</sup>. The way that  $G_0^d$  acts on  $V$  to construct internal multiples suggests the way to remove them. The construction of the first-order<sup>6</sup> internal multiples has the leading-order<sup>7</sup> contribution from the third term of the forward series (Figure 2.1(a)), which suggests that the leading-order<sup>8</sup> contribution to the removal of the first-order internal multiples can be found from the third term in the inverse series (Figure 2.1(b)).

Following that logic, the leading-order contributions to the removal of internal multiples of different orders can be found from different terms in the inverse series. The ISS internal multiple attenuation algorithm (Araujo *et al.*, 1994; Weglein *et al.*, 1997), described here, chooses only the leading order contributions to the removal of internal multiples of all orders from the removal series to form an algorithm that attenuates internal multiples of all orders

---

<sup>5</sup>It takes an infinite number of terms in the forward series to construct internal multiples of each order.

<sup>6</sup>“order” here describes the number of total downward reflections in an internal multiple. For example, an internal multiple with only one downward reflection is called a first-order internal multiple, whereas an internal multiple with two downward reflections is called a second-order internal multiple.

<sup>7</sup>“leading order” contribution in the forward series means the beginning construction of internal multiples of certain order.

<sup>8</sup>“leading order” contribution in the inverse series means the beginning removal of internal multiples of certain order. It takes an infinite number of terms in the inverse series to completely remove internal multiples of each order.

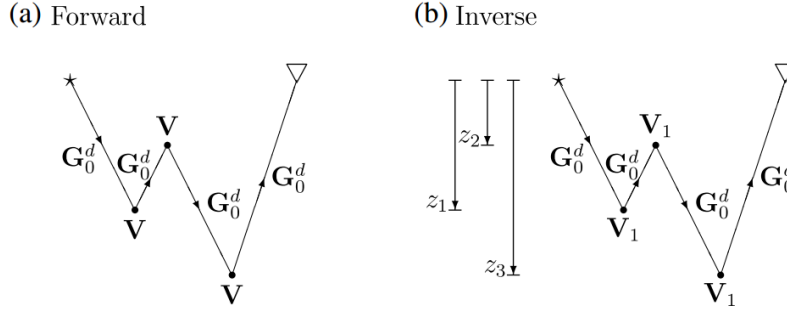


**Fig. 2.1:** The leading order contribution to the generation of first order internal multiples in the forward series is represented in (a) and suggests the leading order contribution to the removal of first order internal multiples in the inverse series in (b). Figure adapted from Weglein *et al.* (2003). Notice that the positive direction of  $z$  axis is downward.

effectively.

The collection of leading-order terms<sup>9</sup> provides the ISS internal multiple attenuation algorithm<sup>10</sup>. The ISS internal multiple attenuation algorithm starts with the input data,  $D(k_g, k_s, \omega)$ , in  $2D$  which is the Fourier transform of the deghosted prestack data with wavelet deconvolved and the free surface multiples removed. The second term,  $D_3(k_g, k_s, \omega)$ , is the leading-order contribution to the removal of the first-order internal multiples. In 2 dimensional case, the second term is  $D_3(k_g, k_s, \omega) = (-2iq_s)^{-1}b_3(k_g, k_s, \omega)$ , where

$$\begin{aligned}
 b_3(k_g, k_s, \omega) = & \frac{1}{(2\pi)^2} \int_{-\infty}^{\infty} dk_1 \int_{-\infty}^{\infty} dk_2 e^{-iq_1(z_g - z_s)} e^{iq_2(z_g - z_s)} \\
 & \times \int_{-\infty}^{\infty} dz_1 b_1(k_g, k_1, z_1) e^{i(q_g + q_1)z_1} \\
 & \times \int_{-\infty}^{z_1 - \epsilon} dz_2 b_1(k_1, k_2, z_2) e^{-i(q_1 + q_2)z_2} \\
 & \times \int_{z_2 + \epsilon}^{\infty} dz_3 b_1(k_2, k_s, z_3) e^{i(q_2 + q_s)z_3}. \tag{2.12}
 \end{aligned}$$

$\omega$  is temporal frequency,  $k_s$  and  $k_g$  are the horizontal wavenumbers for the source and re-

<sup>9</sup>Terms providing those leading-order contributions to the removal of internal multiples of different orders are called leading-order terms.

<sup>10</sup>Because it collects only the leading-order terms, this algorithm is also referred to as leading-order ISS internal multiple attenuation algorithm.

ceiver coordinates, respectively;  $q_g$  and  $q_s$  are the vertical source and receiver wavenumbers defined by  $q_i = \text{sgn}(\omega) \sqrt{\frac{\omega^2}{c_0^2} - k_i^2}$  for  $i \in \{g, s\}$ ;  $z_s$  and  $z_g$  are source and receiver depths; and  $z_j$  ( $i \in \{1, 2, 3\}$ ) represents pseudo-depth using reference velocity migration. The quantity  $b_1(k_g, k_s, z)$  corresponds to Stolt extended Claerbout III migration (Weglein *et al.*, 1997; Weglein, 2016) of effective plane-wave incident data, and  $b_1(k_g, k_s, q_g + q_s) = -2iq_s D(k_g, k_s, \omega)$ . Weglein and Matson (1998) have demonstrated that Equation 2.12 can be interpreted as the subevents prediction of internal multiples. Figure 2.2 illustrates a prediction of a first-order internal multiple by Equation 2.12 using three primary events satisfying “lower-higher-lower” relationship in pseudo-depth domain in the data. This “lower-higher-lower” relationship is carried out by a small positive number  $\epsilon$  in the limits of the integrals. In Equation 2.12, it requires  $z_3 > z_2 + \epsilon$  and  $z_2 < z_1 - \epsilon$ , hence, the relationship “lower( $z_1$ )-higher( $z_2$ )-lower( $z_3$ )”. Notice that,  $z_j$  ( $i \in \{1, 2, 3\}$ ) is pseudo-depth using reference velocity migration, however, the “lower-higher-lower” relationship in real depth is retained in pseudo-depth domain for most cases. Therefore, using this “lower-higher-lower” relationship in pseudo-depth domain will predict the first-order internal multiples with three reflections corresponding to “lower-higher-lower” locations in real depth (Nita and Weglein, 2007).

The predicted internal multiples have accurate time and approximate amplitude compared with the true internal multiples in the data.

With the input data and the leading-order contribution to the removal of the first-order internal multiples, data with the first order internal multiples attenuated are given by

$$D(k_g, k_s, \omega) + D_3(k_g, k_s, \omega). \quad (2.13)$$

Following the same logic of isolating the leading-order contribution to the removal of the first-order internal multiples, leading-order contributions to the removal of higher-order internal multiples (e.g., second-order and third-order internal multiples) can also be identified. With those leading-order contributions to the removal of internal multiples of different or-

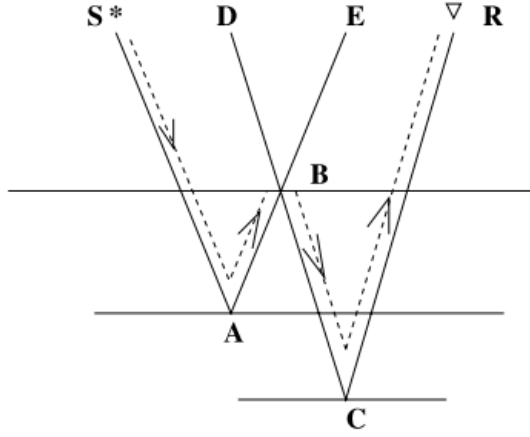


**Fig. 2.2:** Subevents construction of a first-order internal multiples in  $b_3$  in equation 2.12. The first-order internal multiple ( $SABCR$ ) can be constructed using three primary events ( $SAE$ ,  $DCR$  and  $DBE$ ). The accurate time is predicted by  $(SAE)_{time} + (DCR)_{time} - (DBE)_{time} = (SABCR)_{time}$ .

ders, the data with internal multiples of all orders attenuated,  $D^{IM}$ , can be obtained by adding those leading-order contributions to the data itself (Equation 2.14).

$$\begin{aligned}
 D^{IM}(k_g, k_s, \omega) &= \underbrace{D(k_g, k_s, \omega)}_{\text{input data}} + \underbrace{D_3(k_g, k_s, \omega)}_{\substack{\text{leading-order contribution to the} \\ \text{removal of 1st-order internal multiples}}} \\
 &+ \underbrace{D_5(k_g, k_s, \omega)}_{\substack{\text{leading-order contribution to the} \\ \text{removal of 2nd-order internal multiples}}} \\
 &+ \underbrace{\dots}_{\substack{\text{leading-order contribution to the} \\ \text{removal of further higher-order internal multiples}}}, \\
 &= D(k_g, k_s, \omega) + \sum_{n=1}^{\infty} D_{2n+1}(k_g, k_s, \omega), \tag{2.14}
 \end{aligned}$$

where  $D(k_g, k_s, \omega)$  is the input data and  $D_{2n+1}(k_g, k_s, \omega)$  is the leading-order contributions to the removal of  $n^{th}$  order internal multiples ( $n = 1, 2, 3, \dots$ )<sup>11</sup>. In the literature on ISS

<sup>11</sup>Internal multiple attenuation through the Inverse Scattering Series (ISS) is among the most intensive computer processes employed in exploration seismology (Terenghi and Weglein, 2011). In multi-dimensional case, usually only the second-term in equation 2.14 (i.e.  $D_3(k_g, k_s, \omega)$ ) is calculated to attenuate the most

internal multiple attenuation, the  $D_{2n+1}$  term is also referred to as the attenuator of the  $n^{\text{th}}$  order internal multiples.  $D_{2n+1}(k_g, k_s, \omega) = (-2iq_s)^{-1}b_{2n+1}(k_g, k_s, q_g + q_s)$ . A recursive relationship that provides  $b_{2n+1}$  in terms of  $b_{2n-1}$  for  $n = 1, 2, 3, \dots$ , is given as

$$\begin{aligned} b_{2n+1}(k_g, k_s, q_g + q_s) &= \frac{1}{(2\pi)^{2n}} \int_{-\infty}^{\infty} dk_1 e^{-iq_1(\epsilon_g - \epsilon_s)} \\ &\quad \times \int_{-\infty}^{\infty} dz_1 e^{i(q_g + q_1)z_1} b_1(k_g, k_1, z_1) A_{2n+1}(k_1, k_s, z_1), \\ n &= 1, 2, 3, \dots, \end{aligned} \quad (2.15)$$

where

$$\begin{aligned} A_3(k_1, k_s, z_1) &= \int_{-\infty}^{\infty} dk_2 e^{iq_2(\epsilon_g - \epsilon_s)} \int_{-\infty}^{z_1 - \epsilon} dz_2 e^{i(-q_1 - q_2)z_2} b_1(k_1, k_2, z_2) \\ &\quad \times \int_{z_2 + \epsilon}^{\infty} e^{i(q_2 + q_s)z_3} b_1(k_2, k_s, z_3) \end{aligned}$$

and

$$\begin{aligned} A_{2n+1}(k_1, k_s, z_1) &= \int_{-\infty}^{\infty} dk_2 e^{iq_2(\epsilon_g - \epsilon_s)} \int_{-\infty}^{z_1 - \epsilon} dz_2 e^{i(-q_1 - q_2)z_2} b_1(k_1, k_2, z_2) \\ &\quad \times \int_{z_2 + \epsilon}^{\infty} e^{i(q_2 + q_s)z_3} A_{2n-1}(k_2, k_s, z_3), \quad n = 2, 3, 4, \dots \end{aligned}$$

Next, following Weglein *et al.* (2003), I will provide a 1D normal incident analytic example to illustrate the steps to use ISS internal multiple attenuation algorithm predict the first-order internal multiples.

For a 1D earth and a normal incident plane wave, equation 2.13 reduces to (in time domain)

$$D^{IM}(t) = D(t) + D_3(t),^{12} \quad (2.16)$$

---

significant first-order internal multiples.

<sup>12</sup>Inverse Fourier transform takes equation 2.13 in wavenumber-frequency domain to space-time domain. In 1D normal incident case, seismic data D in space-time domain is only a function of time.

and equation 2.12 reduce to

$$b_3(k) = \int_{-\infty}^{\infty} dz_1 e^{ikz_1} b_1(z_1) \int_{-\infty}^{z_1-\epsilon} dz_2 e^{-ikz_2} b_1(z_2) \int_{z_2+\epsilon}^{\infty} dz_3 e^{ikz_3} b_1(z_3). \quad (2.17)$$

where, for a normal incident plane wave,  $D_3(\omega) = b_3(k)$ .

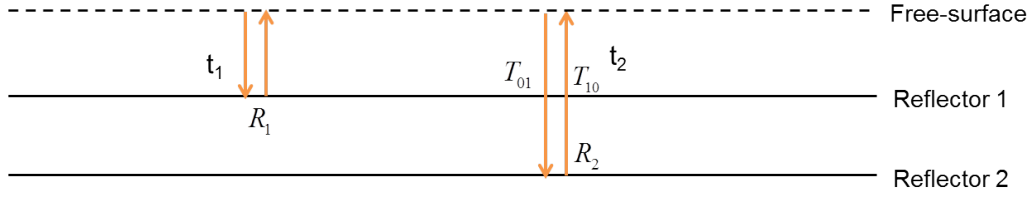


**Fig. 2.3:** A one dimensional model with two reflectors.

In a two-reflector model (see Figure 2.3), the data  $D(t)$  due to a normal incident wave are

$$D(t) = R_1 \delta(t - t_1) + R'_2 \delta(t - t_2) + \dots, \quad (2.18)$$

where  $R'_2 = T_{01} R_2 T_{10}$ .  $R_1$  and  $R_2$  are the reflection coefficients of the first and second reflector, respectively.  $T_{01}$  and  $T_{10}$  are transmission coefficients across the reflector 1.

A temporal Fourier transform of  $D(t)$  gives the data in the frequency domain,

$$D(\omega) = R_1 e^{i\omega t_1} + R'_2 e^{i\omega t_2} + \dots. \quad (2.19)$$

For a 1D medium and a normal incident plane wave,  $D(\omega) = b_1(k_z)$  and the vertical wave number is  $k_z = \frac{2\omega}{c_0}$ . Then, the reflection data can be expressed in terms of  $k_z$ ,

$$b_1(k_z) = R_1 e^{i \frac{2\omega}{c_0} \frac{c_0 t_1}{2}} + R'_2 e^{i \frac{2\omega}{c_0} \frac{c_0 t_2}{2}} + \dots. \quad (2.20)$$

Define the pseudo-depths  $z_1$  and  $z_2$  in the reference medium as  $z_1 \equiv \frac{c_0 t_1}{2}$  and  $z_2 \equiv \frac{c_0 t_2}{2}$ ,

respectively. Rewrite the data as,

$$b_1(k) = R_1 e^{ik_z z_1} + R'_2 e^{ik_z z_2} + \dots \quad (2.21)$$

After performing the Inverse Fourier transform from  $k_z$  to  $z$ ,  $b_1(z) = \int_{-\infty}^{\infty} e^{-ik_z z} b(k_z) dz$ , substituting the data into the algorithm 2.17, and Fourier transforming back to the time domain, we have

$$\begin{aligned} D_3(t) &= R_1 R_2'^2 \delta(t - (2t_2 - t_1)) + \dots \\ &= R_1 R_2^2 T_{01}^2 T_{10}^2 \delta(t - (2t_2 - t_1)) + \dots \end{aligned} \quad (2.22)$$

Figure 2.4 shows three subevents that are combined to predict the first-order internal multiple. The predicted internal multiple has the accurate phase ( $2t_2 - t_1 = t_2 - t_1 + t_2$ ) and approximate amplitude ( $R_1 R_2^2 T_{01}^2 T_{10}^2 = T_{01} R_2 T_{10} \times R_1 \times T_{01} R_2 T_{10}$ ). The true first-order internal multiple in the data is  $-R_1 R_2^2 T_{01} T_{10} \delta(t - (2t_2 - t_1))$  (Figure 2.5).

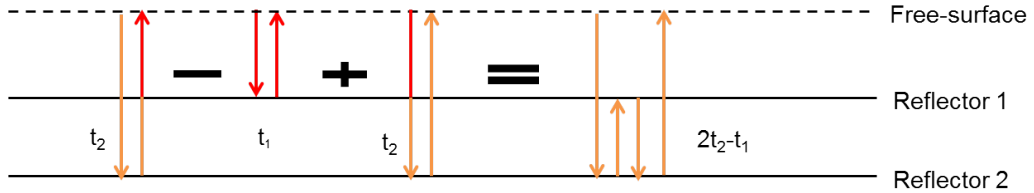


**Fig. 2.4:** Three primary subevents on the left are combined to predict a first-order internal multiple on the right.

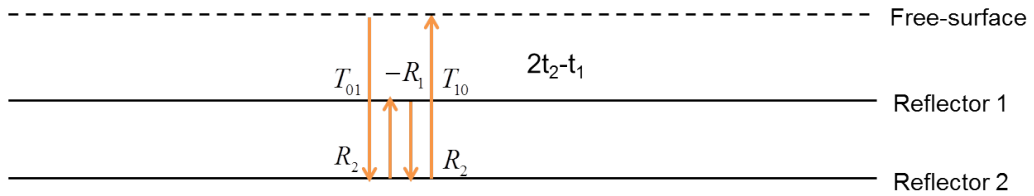


**Fig. 2.5:** The first-order internal multiple in the one dimensional model with two reflectors.

The prediction result has two extra transmission coefficients of  $T_{01}T_{10}$  and an opposite polarity compared with the true internal multiple in the data. Adding the prediction result to the data itself (i.e.,  $D(t) + D_3(t)$ ) attenuates the first-order internal multiple in the data.

Early work of Araújo (1994) and Weglein *et al.* (1997) focused exclusively on the analysis of the leading-order contribution to the removal of internal multiples of all orders (i.e., Equation 2.14) by treating primaries in the data as subevents. However, the input data contain not only primaries but also internal multiples. Zhang and Shaw (2010) have used analytic data from a two-reflector example in 1D normal incident case show that the attenuator of the first-order internal multiple (i.e., Equation 2.12) predicts not only the first-order internal multiples but also higher-order internal multiples when both primaries and internal multiples are treated as subevents. Furthermore, the situation is considerably more complicated when the data from three or more reflectors are considered. In the later case, spurious events can be generated whose traveltimes do not correspond to any physical events in the data. In the next chapter, I will analysis the general output from the current leading-order internal multiple attenuation algorithm (in specific, the general output from the second term in the algorithm, which is the attenuator of the first-order internal multiples) when both primaries and internal multiples enter the algorithm. The general output from the attenuator of the first-order internal multiples includes (1) the prediction of all first-order internal multiples (used to attenuate all the first-order internal multiples in the data), (2) the prediction of all higher-order internal multiples, and (3) non-physical events when the data from three or more reflectors are considered and certain timing relationship occurs. I will demonstrate that the prediction of all higher-order internal multiple will benefit the attenuation of all higher-order internal multiples in the data, and non-physical events are anticipated by higher-order terms in the series and higher-order terms can be included to the current leading-order algorithm to precisely address the non-physical events.

### 3. THE ISS DATA COMPREHENSIVE INTERNAL-MULTIPLE-ATTENUATION ALGORITHM THAT ACCOMMODATES PRIMARIES AND INTERNAL MULTIPLES AS SUBEVENTS IN THE INPUT DATA

The ISS internal-multiple-removal subseries has the promise that, given the input data consisting of primaries and internal multiples, it will output primaries for migration and inversion steps. Early analysis of the ISS internal-multiple-removal subseries focused on identifying leading-order terms from the subseries to develop an ISS internal-multiple-attenuation algorithm (Araujo *et al.*, 1994; Weglein *et al.*, 1997). The algorithm selects three events in the input data by a “longer-shorter-longer” relationship in the vertical-travel-time domain and the *primaries* selected in that procedure predict the accurate time and approximate amplitude of all first-order internal multiples without any subsurface information (Weglein *et al.*, 2003).

However, the input data contain both *primaries* and *internal multiples*. When internal multiples themselves are selected in that procedure, two different types of events will be produced. The first type is higher-order internal multiples (e.g., second-order internal multiples (Zhang and Shaw, 2010)) and the second type is spurious events (events that do not exist in the data).

In this chapter, I will first review the two-reflector analytic example of Zhang and Shaw (2010) and use that analytic example demonstrate that the prediction of higher-order internal multiples is a benefit and definite asset in that these predicted higher-order internal

multiples cooperatively assist and benefit the attenuation of higher-order internal multiples in the data. After that, I will proceed to examine the reason of spurious events generation and the circumstances under which the spurious events issue is significant. I will show that the spurious events are fully anticipated by the ISS, and specific higher-order terms from ISS will precisely address that spurious-event issue. The inclusion of higher-order terms to the original algorithm provides the new ISS data comprehensive internal-multiple-attenuation algorithm that does not generate the spurious events and, at the same time, retains the strength of the original algorithm.

### 3.1 General output from $b_3$ in a two reflector example (Zhang and Shaw, 2010)

Following Zhang and Shaw (2010), I use a two-reflector example illustrate the generation of higher-order internal multiples in the attenuator of the first-order internal multiples in 1D normal incident case. The reflection data due to an impulsive incident wave for a two reflector model (see Figure 3.1) are

$$D(t) = R_1\delta(t - t_1) + R'_2\delta(t - t_2) + R'_4\delta(t - (2t_2 - t_1)) + \dots, \quad (3.1)$$

where  $R'_2 = T_{01}R_2T_{10}$ , and  $R'_4 = T_{01}R_2(-R_1)R_2T_{10}$ .  $R_1$ ,  $R_2$ ,  $T_{01}$  and  $T_{10}$  have the same meaning as in equation 2.18. Note that, in addition to two primaries, I include a first-order internal-multiple in the data (the blue term).

A temporal Fourier transform of  $D(t)$  gives the data in the frequency domain,

$$D(\omega) = R_1e^{i\omega t_1} + R'_2e^{i\omega t_2} + R'_4e^{i\omega(2t_2-t_1)} + \dots. \quad (3.2)$$

For a 1D medium and a normal incident plane wave,  $D(\omega) = b_1(k)$  and the vertical wave

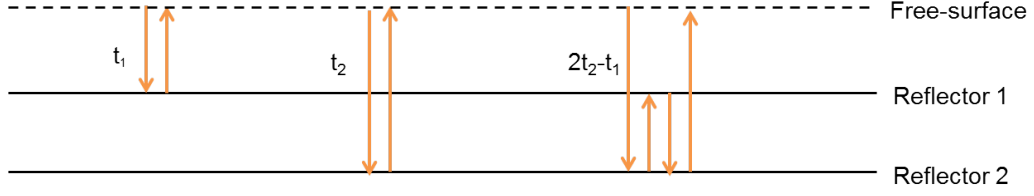


**Fig. 3.1:** A one dimensional model with two reflectors. There are two primaries and one first-order internal multiple shown in the figure.

number is  $k = \frac{2\omega}{c_0}$ . Then, the reflection data can be expressed in terms of  $k$ ,

$$b_1(k) = R_1 e^{i\frac{2\omega}{c_0} \frac{c_0 t_1}{2}} + R'_2 e^{i\frac{2\omega}{c_0} \frac{c_0 t_2}{2}} + R'_4 e^{i\frac{2\omega}{c_0} \frac{c_0(2t_2-t_1)}{2}} + \dots \quad (3.3)$$

Define the pseudo-depths  $z_1$  and  $z_2$  in the reference medium as  $z_1 \equiv \frac{c_0 t_1}{2}$  and  $z_2 \equiv \frac{c_0 t_2}{2}$ , respectively. Rewrite the data as,

$$b_1(k) = R_1 e^{ikz_1} + R'_2 e^{ikz_2} + R'_4 e^{ik(2z_2-z_1)} + \dots \quad (3.4)$$

After performing the Inverse Fourier transform from  $k$  to  $z$ ,  $b_1(z) = \int_{-\infty}^{\infty} e^{-ikz} b_1(k) dz$ ,

$$b_1(z) = R_1 \delta(z - z_1) + R'_2 \delta(z - z_2) + R'_4 \delta(z - (2z_2 - z_1)) + \dots \quad (3.5)$$

substituting the data into the algorithm  $b_3(k)$ , and Fourier transforming back to the time domain (in this case,  $b_3(k) = D_3(\omega)$ ),

$$\begin{aligned} D_3(t) = & R_1 R_2'^2 \delta(t - (2t_2 - t_1)) + 2R_1 R_2' R_4' \delta(t - (3t_2 - 2t_1)) \\ & + R_2' R_4'^2 \delta(t - (3t_2 - 2t_1)) + R_1 R_4'^2 \delta(t - (4t_2 - 3t_1)) + \dots \end{aligned} \quad (3.6)$$

Result 3.6 shows that the prediction includes (1) the first-order internal multiples (the blue term) and (2) higher-order internal multiples (the red terms).

Similar to Figure 2.4, Figure 3.2 explains the prediction of a higher-order internal multiple ( $2R_1R_2R_4'\delta(t - (3t_2 - 2t_1))$ ) in  $b_3$  by combining not only primaries but also internal multiples in the input data as subevents. The factor of 2 in the prediction coefficient is because the first-order internal multiple can act as a subevents in either the innermost or outermost integral in  $b_3$ .

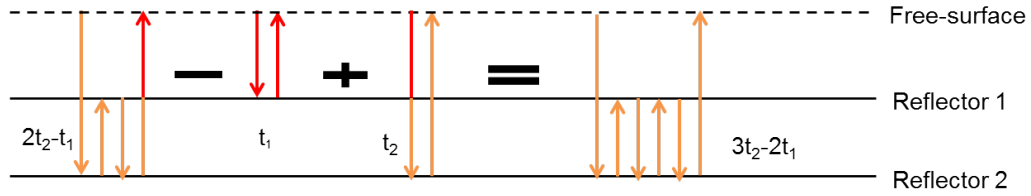


**Fig. 3.2:** One internal multiple subevent and two primary subevents on the left are combined to predict a second-order internal multiple on the right.

Therefore, not only the first-order internal multiples but also the higher-order internal multiples are predicted when both primary events and internal multiple events are combined as subevents in  $D_3$ .

In the following, I will demonstrate that these predicted higher-order internal multiples benefit the attenuation of higher-order internal multiples in the data. In other words, the second term of the ISS internal multiple attenuation algorithm ( $D_3$ ) has the specific role of (1) predicting all the first-order internal multiples (used to attenuate the first-order internal multiples in the data) and (2) predicting all higher-order internal multiples (used to benefit attenuating higher-order internal multiples in the data, as this section will show in the following).

The property of each term within a subseries having specific roles and different terms working cooperatively to achieve the specific task associated with that subseries is referred to as purposeful perturbation (Weglein *et al.*, 2003). The fact that,  $D_3$  benefits the attenuation of higher-order internal multiples in the data together with subsequent terms (e.g.,  $D_5$  and  $D_7$ ), demonstrates the property of purposeful perturbation in the ISS internal multiple

attenuation subseries.

Before I show the property of purposeful perturbation in the ISS internal multiple case, I will first review an example of purposeful perturbation in the ISS free-surface multiple case, and then compares the analogous and different points.

### 3.1.1 Example of purpose perturbation in the ISS free-surface multiple removal case

Following Weglein *et al.* (2003), I illustrate the purposeful perturbation in ISS free-surface removal case using a 1D normal incident example. In a 1D earth with a normal incident plane wave and a source wavelet with a unit amplitude, i.e.,  $B(\omega) = 1$ , the algorithm can be written as (Weglein *et al.*, 2003):

$$\begin{aligned} R &= \frac{R_{FS}}{1 - R_{FS}} \\ &= R_{FS} + R_{FS}^2 + R_{FS}^3 + \dots, \end{aligned} \tag{3.7}$$

where  $R_{FS}$  and  $R$  are data with and without free-surface multiples, respectively. Notice that the free-surface is characterized by a reflection coefficient of -1 for a pressure wavefield. Similarly, I can consider the second term in equation 3.7 as the prediction of the first-order free-surface multiples and the third term as the prediction of the second-order free-surface multiples, etc.

I use a 1D analytic example to illustrate the prediction of the free-surface multiples. The model (Figure 3.3) has two reflectors, and the input data (Equation 3.8) with two primaries (black terms), three first-order (blue terms) and four second-order (red terms) free-surface

multiples, can be written as:

$$\begin{aligned}
R_{FS}(t) = & R_1\delta(t - t_1) + R'_2\delta(t - t_2) - R_1^2\delta(t - 2t_1) - R_2'^2\delta(t - 2t_2) - 2R_1R'_2\delta(t - t_1 - t_2) \\
& + R_1^3\delta(t - 3t_1) + R_2'^3\delta(t - 3t_2) + 3R_1R_2'^2\delta(t - t_1 - 2t_2) + 3R_1^2R'_2\delta(t - 2t_1 - t_2) + \dots,
\end{aligned} \tag{3.8}$$

where  $R_1$  and  $R'_2$  are amplitudes of the first and second primaries, respectively.  $R'_2 = T_{01}R_2T_{10}$ . The assumption is the downward reflection coefficient at the free-surface to be -1.

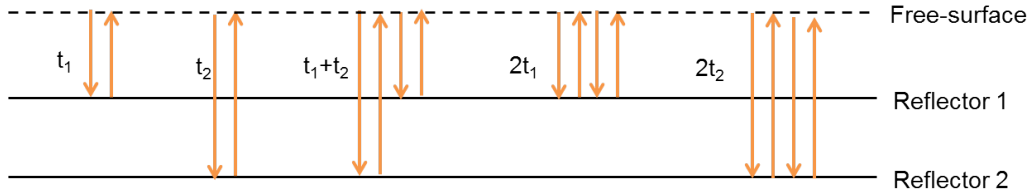


**Fig. 3.3:** A one dimensional model with two reflectors. Notice that, the figure only shows two primaries and three first-order free-surface multiples.

In the temporal frequency domain, the data are

$$\begin{aligned}
R_{FS}(\omega) = & R_1e^{i\omega t_1} + R'_2e^{i\omega t_2} - R_1^2e^{i\omega 2t_1} - R_2'^2e^{i\omega 2t_2} - 2R_1R'_2e^{i\omega(t_1+t_2)} \\
& + R_1^3e^{i\omega 3t_1} + R_2'^3e^{i\omega 3t_2} + 3R_1^2R'_2e^{i\omega(2t_1+t_2)} + 3R_1R_2'^2e^{i\omega(t_1+2t_2)} + \dots.
\end{aligned} \tag{3.9}$$

With equation 3.9, the second and third terms in equation 3.7 are

$$\begin{aligned}
R_{FS}^2(\omega) = & R_1^2e^{i\omega 2t_1} + R_2'^2e^{i\omega 2t_2} + 2R_1R'_2e^{i\omega(t_1+t_2)} \\
& - 6R_1R_2'^2e^{i\omega(t_1+2t_2)} - 6R_1^2R'_2e^{i\omega(2t_1+t_2)} - 2R_1^3e^{i\omega 3t_1} - 2R_2'^3e^{i\omega 3t_2} + \dots,
\end{aligned} \tag{3.10}$$

and

$$R_{FS}^3(\omega) = R_1^3 e^{i\omega 3t_1} + R_2^3 e^{i\omega 3t_2} + 3R_1 R_2' e^{i\omega(t_1+2t_2)} + 3R_1^2 R_2' e^{i\omega(2t_1+t_2)} + \dots, \quad (3.11)$$

respectively.

From equation 3.10, It is concluded that (e.g., Weglein *et al.* (2003)) when  $R_{FS}^2(\omega)$  is added to  $R_{FS}(\omega)$ , two things happen: (1) The first-order free-surface multiples are eliminated (blue terms in equations 3.9 and 3.10 cancel each other) and (2) Higher-order free-surface multiples are altered. Together with  $R_{FS}^3(\omega)$ , second-order free-surface multiples are eliminated (red terms in equations 3.9, 3.10 and 3.11 cancel each other) as shown in equation 3.12.

$$\begin{aligned} R_{FS}(\omega) : & \quad 1 \times [R_1^3 e^{i\omega 3t_1} + R_2^3 e^{i\omega 3t_2} + 3R_1^2 R_2' e^{i\omega(2t_1+t_2)} + 3R_1 R_2'^2 e^{i\omega(t_1+2t_2)}] \\ R_{FS}^2(\omega) : & \quad -2 \times [R_1^3 e^{i\omega 3t_1} + R_2^3 e^{i\omega 3t_2} + 3R_1^2 R_2' e^{i\omega(2t_1+t_2)} + 3R_1 R_2'^2 e^{i\omega(t_1+2t_2)}] \\ R_{FS}^3(\omega) : & \quad 1 \times [R_1^3 e^{i\omega 3t_1} + R_2^3 e^{i\omega 3t_2} + 3R_1 R_2'^2 e^{i\omega(t_1+2t_2)} + 3R_1^2 R_2' e^{i\omega(2t_1+t_2)}] \end{aligned} \quad (3.12)$$

The alteration in  $R_{FS}^2(\omega)$  prepares for the elimination of second-order free-surface multiples using  $R_{FS}^3(\omega)$ .

Next, we further categorize the results as follows. Consider the input data containing primary and free-surface multiples, i.e.,

$$R_{FS}(\omega) = P + F,$$

where  $P$  and  $F$  stand for primaries and free-surface multiples, respectively.

Therefore,  $R_{FS}^2(\omega)$  can be expressed as

$$R_{FS}^2(\omega) = (P + F)^2 = PP + PF + FP + FF.$$

Under this categoration, the blue and red terms in equation 3.10 come from combinations of  $PP$  and  $PF$  (or  $FP$ ) terms, respectively. Together with the 1D analytic example, we conclude that the  $PP$  combination in  $R_{FS}^2(\omega)$  is used to eliminate the first-order free-surface multiples, whereas the  $PF$  (or  $FP$ ) combination in  $R_{FS}^2(\omega)$  is used to alter and benefit the elimination of the second-order free-surface multiples.

In this part, I use a 1D analytic example to exemplify the necessity of including both primaries and free-surface multiples in the input of the ISS free-surface multiple elimination algorithm in order to completely eliminate the free-surface multiples. Within the analytic example, the ISS free-surface elimination algorithm demonstrates the collaborative nature among the different terms in collectively fulfilling the task. It is interesting that the ISS free-surface-multiple elimination algorithm anticipates that there are both primaries and free-surface multiples as input and uses both of them to achieve that task. In the next part, I will use a two-reflector example to discuss an analogous feature in the ISS internal-multiple-attenuation case, and I will analyze the difference between these two cases.

### 3.1.2 Example of purposeful perturbation in the ISS internal multiple attenuation case

In this part, I will use a normal incident example in 1D earth to illustrate the cooperative nature between different terms in ISS internal multiple attenuation algorithm.

Also, to categorize the result, consider the input data containing primaries and internal multiples, i.e.,

$$b_1 = P + I,$$

where  $P$  and  $I$  stand for primaries and internal multiples, respectively. The prediction

result of the attenuator of the first-order internal multiples is

$$\begin{aligned}
b_3 &= b_1 * b_1 * b_1 \\
&= (P + I)(P + I)(P + I) \\
&= PPP + PPI + PIP + IPP + PII + IPI + IIP + III, \tag{3.13}
\end{aligned}$$

where  $*$  represents the non-linear combination between data. Further analysis shows that the prediction of the first-order internal multiples (the blue term in equation 3.6) results from  $PPP$  combinations and prediction of all other higher-order internal multiples (red terms in equation 3.6) results from  $PPI$  (or  $IPP$  or  $IPI$ ) combinations.

To summarize analogous points in the free-surface multiple and internal multiple cases: (1) both first-order and higher-order multiples are predicted in  $R_{FS}^2$  and or  $b_3$ ; and (2) higher-order multiples are predicted because of the lower-order multiples in the input data entering as subevents.

In last part, it was shown that the second-order free-surface multiples predicted by  $R_{FS}^2(\omega)$  are used to eliminate the second-order free-surface multiple, see equation 3.12. Next, I will show the second-order internal multiples predicted by  $D_3$  (the first two red terms in 2.22) will assist and benefit the attenuating of second-order internal multiples in the seismic data.

Let's first examine the prediction result from the attenuator of second-order internal multiples (i.e., equation 2.15 when  $n = 2$ ). For 1D normal incident spike date, it is

$$\begin{aligned}
b_5(k) &= \int_{-\infty}^{\infty} dz_1 e^{ikz_1} b_1(z_1) \int_{-\infty}^{z_1-\epsilon} dz_2 e^{-ikz_2} b_1(z_2) \int_{z_2+\epsilon}^{\infty} dz_3 e^{ikz_3} b_1(z_3) \\
&\quad \times \int_{-\infty}^{z_3-\epsilon} dz_4 e^{ikz_4} b_1(z_4) \int_{z_4+\epsilon}^{\infty} dz_5 e^{-ikz_5} b_1(z_5). \tag{3.14}
\end{aligned}$$

Given equation 3.14, the prediction result using the same input data (equation 3.1) is

$$D_5(t) = R_2^3 R_1^2 \delta(t - (3t_2 - t_1)) + \dots = T_{01}^3 T_{10}^3 R_2^3 R_1^2 \delta(t - (3t_2 - 2t_1)) + \dots . \quad (3.15)$$

This is the prediction of the second-order internal-multiple from the attenuator of the second-order internal multiples.

To summarize, the actual second-order internal multiple in the data  $D(t)$ , the second-order internal-multiple prediction in  $D_3(t)$ , and  $D_5(t)$  are

$$\begin{aligned} D(t) : & & & 1 \times [T_{01} T_{10} R_2^3 R_1^2 \delta(t - (3t_2 - 2t_1))], \\ D_3(t) : & & (-2T_{01} T_{10} + (T_{01} T_{10} R_1)^2) \times [T_{01} T_{10} R_2^3 R_1^2 \delta(t - (3t_2 - 2t_1))], \\ D_5(t) : & & (T_{01} T_{10})^2 \times [T_{01} T_{10} R_2^3 R_1^2 \delta(t - (3t_2 - 2t_1))], \end{aligned} \quad (3.16)$$

respectively. Comparing equations 3.12 and 3.16, I find analogous roles of the higher-order internal-multiple prediction in  $D_3(t)$ , i.e., the prediction of the second-order internal multiples by  $D_3(t)$  assists and benefits the attenuating of higher internal multiples in the data.

Similar to the ISS free-surface multiple removal case, the ISS internal multiple attenuation algorithm anticipates that both the primaries and internal multiples will be the input, and uses both types of events to attenuate internal multiples in the data.

Next, we show a numerical example in 1D case to demonstrate the purposeful perturbation between different terms in the ISS internal multiple attenuation algorithm to collectively achieve the attenuation of internal multiples. Figure 3.4 shows the test data we use (shown in the pseudo-depth domain). Figure 3.5a, 3.5b and 3.5c shows the comparison between the input data (before attenuating internal multiples) and the output data (after attenuating internal multiples) when adding different prediction terms in equation 2.16.

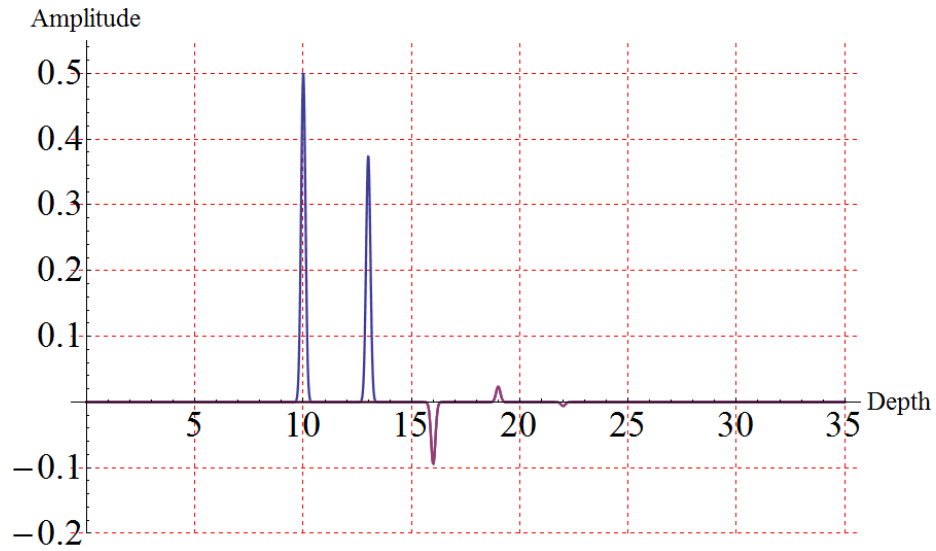


**Fig. 3.4a:** Input data in pseudo-depth domain. Blue and purple lines represent primaries and internal multiples, respectively. There are two primaries at depths 10 and 13 and three internal multiples at pseudo-depths 16 (first-order), 19 (second-order), and 22 (third-order).

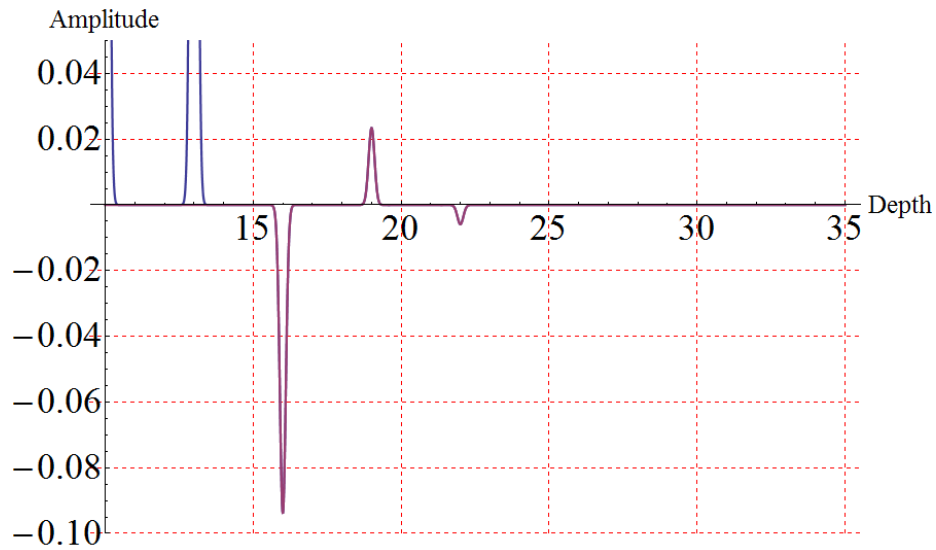


**Fig. 3.4b:** A zoom-in of Figure 3.4a in the range of 10 – 35.



**Fig. 3.5a:** Comparison between  $D$  (blue) and  $D + D_3$  (purple). The comparison shows the contributions of  $D_3$  are (1) reducing the first-order internal multiples and (2) altering the amplitude of the higher-order internal multiples. Notice that, only internal multiples are plotted in  $D$ .

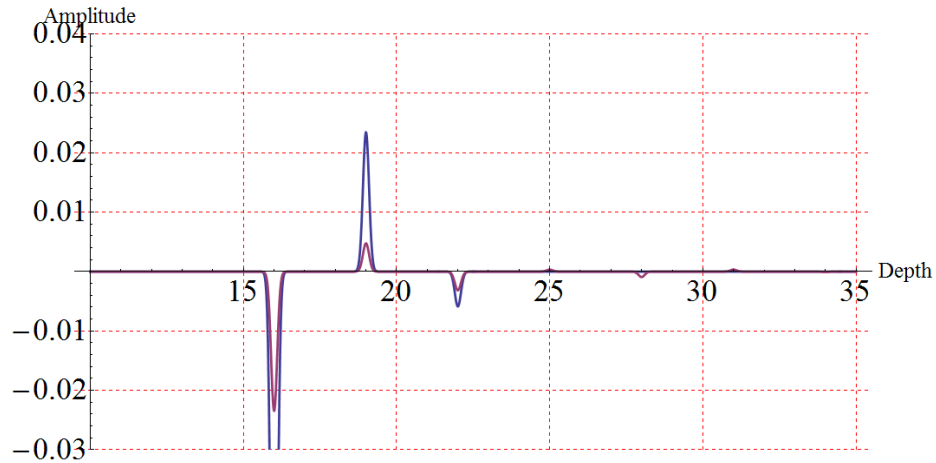


**Fig. 3.5b:** Comparison between  $D$  (blue) and  $D + D_3 + D_5$  (purple). Adding  $D_5$  to  $D + D_3$  will further reduce second-order internal multiple.

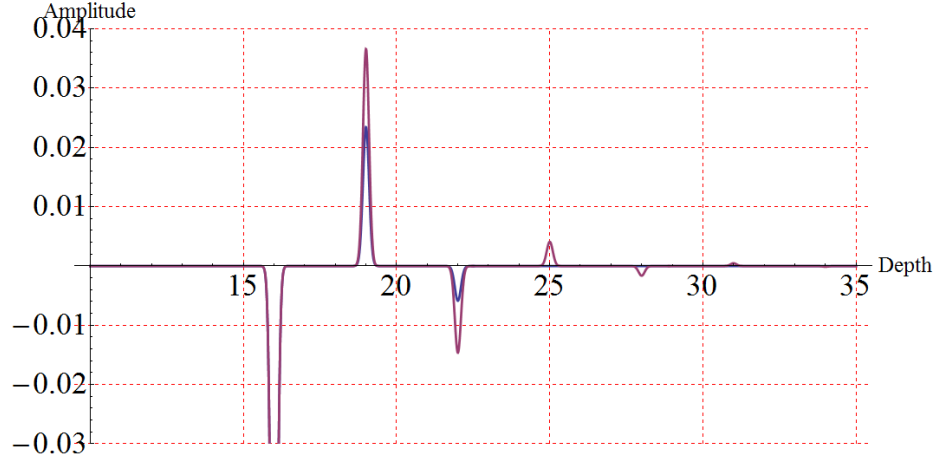


**Fig. 3.5c:** Comparison between  $D$  (blue) and  $D + D_5$  (purple). Without the contribution from  $D_3$ ,  $D + D_5$  will **increase** the amplitude of the second-order internal multiple. In other words, alteration of higher-order internal multiples by  $D_3$  is necessary for their attenuation.

### 3.2 General output from $b_3$ in a three or more reflector example

In the last section, I use both analytic example and numerical example in a two-reflector model analyze the general output from the attenuator of the first-order internal multiples. In this section, I proceed to examination of a more complicated case where data is generated from a three-reflector model (Figure 3.6). In this example, I include one more primary from the third reflector in the input data.

$$D(t) = R_1\delta(t - t_1) + R_2'\delta(t - t_2) + R_4'\delta(t - (2t_2 - t_1)) + R_3'\delta(t - t_3) + \dots, \quad (3.17)$$

where  $R_2'$  and  $R_4'$  are the same as in equation 3.1, and  $R_3' = T_{01}T_{12}R_3T_{21}T_{10}$  is the amplitude of the third primary.

Given these data, following the same procedure from equation 3.1 to equation ??, the

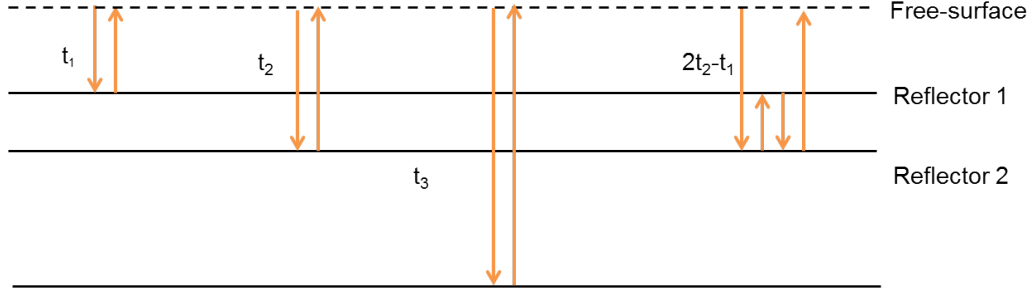


**Fig. 3.6:** A one dimensional model with two reflectors. There are two primaries and one first-order internal multiple shown in the figure.

prediction result from the attenuator of the first-order internal multiples is:

$$\begin{aligned}
D_3(t) = & R_1(R'_2)^2\delta(t - (2t_2 - t_1)) + 2R_1R'_2R'_3\delta(t - (t_2 + t_3 - t_1)) \\
& + R_1(R'_3)^2\delta(t - (2t_3 - t_1)) + R_2(R'_3)^2\delta(t - (2t_3 - t_2)) \\
& + 2R_1R'_2R'_4\delta(t - (3t_3 - 2t_1)) + R'_2(R'_4)^2\delta(t - (3t_3 - 2t_2)) \\
& + 2R_1R'_3R'_4\delta(t - (t_3 + 2t_2 - 2t_1)) + R_1(R'_4)^2\delta(t - (4t_2 - 3t_1)) \\
& + 2R'_2R'_3R'_4\delta(t - (t_3 + t_2 - t_1)) \\
& + (R'_3)^2R'_4\delta(t - (2t_3 - (2t_2 - t_1))).
\end{aligned} \tag{3.18}$$

Similarly to result 3.6, result 3.18 has the predictions of the first-order internal multiples (blue terms) and higher-order internal multiples (red terms). However, the last term is neither a primary nor an internal multiple. This prediction is called a spurious event. Further examination shows that this spurious event results from the *PIP* combination (Figure 3.7), hence, this type of spurious events (caused by “primary-internal multiple-primary”) is denoted as *PIP* type spurious events. Notice that, I assume  $2t_2 - t_1 < t_3$  in deriving result 3.18. This assumption is required by “lower-higher-lower” relationship to combine “primary ( $t_3$ )-internal multiple ( $2t_2 - t_1$ )-primary ( $t_3$ )” in  $b_3$ .

Figure 3.7 illustrates the simplest case where a *PIP* type spurious event can happen. This

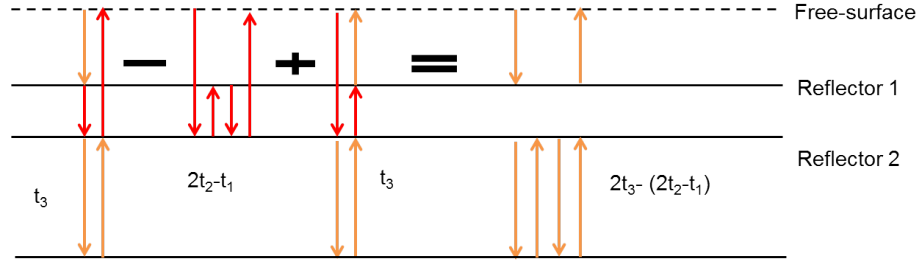


**Fig. 3.7:** In a three-reflector example, a “primary-internal multiple-primary” can be combined to produce a spurious prediction.

type of spurious events can be produced when there are three or more reflectors and certain timing relationship occurs (e.g.,  $2t_2 - t_1 < t_3$  in Figure 3.7).

Besides the *PIP* type of spurious events, other types of spurious events exist (Liang *et al.*, 2013). For example, Figure 3.8 illustrates a case where a *PPI* type spurious event (caused by “primary-primary-internal multiple”). Similarly, it can be shown that this type of spurious events can be produced when there are four or more reflectors and certain timing relationship occurs (e.g.,  $2t_2 - t_1 > t_3$  in Figure 3.8)

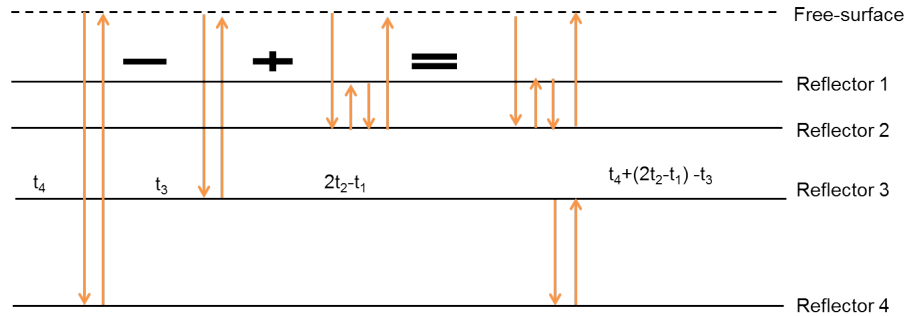


**Fig. 3.8:** In a four-reflector example, a “primary-primary-internal multiple” can be combined to produce a spurious prediction.

It can be shown that additional types of spurious events can be generated when two internal multiple subevents (e.g., “primary-internal multiple-internal multiple”, denoted by *PII*) or three internal multiple subevents (“internal multiple-internal multiple-internal multiple”, denoted by *III*) are combined by the attenuator of the first-order internal multiples.

To summarize the general output from the attenuator of the first-order internal multiples (i.e.,  $D_3$ ) when both primaries and internal multiples are present in the data and combined by the attenuator, the general output consists of

1. prediction of all first-order internal multiples (used to attenuate all first-order internal multiples in the input data);
2. prediction of all higher-order internal multiples (used to benefit and assist the attenuation of all higher-order internal multiples in the input data, together with prediction of higher-order internal multiples from subsequent terms, e.g.,  $D_5$  and  $D_7$ );
3. spurious events when the input data is generated from a three or more reflector model and certain timing relationship occurs.

As it was demonstrated in the previous section, the ISS internal-multiple-removal subseries anticipates that both primaries and internal multiple are present in the input of the current leading-order ISS internal multiple attenuation algorithm and uses both of them to attenuate internal multiples of all orders by collectively cooperation between different terms, the ISS internal multiple removal subseries also anticipates spurious events can be produced from this leading-order algorithm and higher-order terms from the subseries can be identified to precisely address the spurious events generation.

### **3.3 An ISS data comprehensive internal-multiple-attenuation algorithm that accommodates primaries and internal multiples in the input data**

Higher-order terms can be identified from the ISS internal-multiple-removal subseries to address the spurious events. Including these higher-order terms to the current leading-order algorithm provides a data comprehensive ISS internal multiple attenuation algorithm

removes the generation of spurious events and, at the same time, retains the unique effectiveness of current algorithm<sup>1</sup>.

Guided by the origin of spurious events, higher-order terms are identified to precisely address the spurious events. For example, to address a spurious events generated by combining “primary-internal multiple-primary”, a portion of the fifth order term from the ISS ( $G_0V_1G_0V_3G_0V_1G_0$ ) can be employed to address the *PIP* spurious events. In 1D normal incident case, it was expressed as follows

$$b_5^{PIP}(k) = \int_{-\infty}^{\infty} dz_1 e^{ikz_1} b_1(z_1) \int_{-\infty}^{z_1-\epsilon} dz_2 e^{-ikz_2} b_3(z_2) \int_{z_2+\epsilon}^{\infty} dz_3 e^{ikz_3} b_1(z_3), \quad (3.19)$$

where  $b_1(z)$  is has the same meaning as that in equation 2.17 and  $b_3(z)$  is the attenuator of the first-order internal multiples expressed in pseudo-depth domain in 1D normal incident case. The superscript on the left hand side of this equation (i.e., *PIP*) represents this higher-order term is used to address the spurious events generated by “primary-internal multiple-primary”.

Including term  $b_5^{PIP}$  to the current algorithm provides the benefit of the original algorithm while addressing issues due to spurious events

$$D^{IM}(t) = D(t) + D_3(t) + D_5^{PIP}(t), \quad (3.20)$$

where  $D_5^{PIP}(t)$  is the Inverse Fourier transform of  $D_5^{PIP}(\omega)$ , and  $D_5^{PIP}(\omega) = b_5^{PIP}(k)$ .

Compared with the original algorithm (equation 2.16), the new algorithm includes a portion of the higher order term ( $b_5^{PIP}$ ) to address the *PIP* spurious events.

Using the same logic and analysis, other higher-order terms are identified to address other types of spurious events. For example,  $b_5^{PPI}$  is identified to address the spurious events

---

<sup>1</sup>For the scope of this dissertation, the data comprehensive algorithm focuses on attenuating all first-order internal multiples and addressing the generation of spurious events.

generated by “primary-primary-internal multiple”.

$$b_5^{PPI}(k) = 2 \int_{-\infty}^{\infty} dz_1 e^{ikz_1} b_1(z_1) \int_{-\infty}^{z_1-\epsilon} dz_2 e^{-ikz_2} b_1(z_2) \int_{z_2+\epsilon}^{\infty} dz_3 e^{ikz_3} b_3(z_3), \quad (3.21)$$

Since this type of spurious event could be produced by the attenuator using a first-order internal multiple subevent in either of the outer integrals (these two cases are equivalent), there is a coefficient 2 in the equation.

It can be shown that, after including all terms used to address different types of spurious events to the current algorithm, the new data comprehensive algorithm boils down to the same form as the current algorithm. The new algorithm that attenuates all first-order internal multiples in the data and addresses spurious events can be expressed, in 1D normal incident case, as follows

$$\begin{aligned} \mathcal{D}^{IM}(t) &= D(t) + \underbrace{D_3(t) + D_5^{PIP}(t) + D_5^{PPI}(t) + \dots}_{\mathcal{D}_3(t)}, \\ &= D(t) + \mathcal{D}_3(t), \end{aligned} \quad (3.22)$$

where  $D(t)$  is the input data consisting of primaries and internal multiples,  $\mathcal{D}_3(t)$  is the prediction of all first-order internal multiples with the addressing of spurious events, and  $\mathcal{D}^{IM}(t)$  is the output data with both all the first-order internal multiples attenuated and spurious events addressed.

Mathematically, it is equivalent to compute  $\mathcal{D}_3(t)$  directly from  $\mathcal{D}_3(\omega) = b_3^{New}(k)$ , where

$$\begin{aligned} b_3^{New}(k) &= \int_{-\infty}^{\infty} dz_1 e^{ikz_1} [b_1(z_1) + b_3(z_1)] \int_{-\infty}^{z_1-\epsilon} dz_2 e^{-ikz_2} [b_1(z_2) + b_3(z_2)] \\ &\quad \times \int_{z_2+\epsilon}^{\infty} dz_3 e^{ikz_3} [b_1(z_3) + b_3(z_3)]. \end{aligned} \quad (3.23)$$

In equation 3.23,  $b_1(z)$  and  $b_3(z)$  has the same meaning as in equation 2.17. Notice that

equation 3.23 and equation 2.17 have the same form but different integrand. Equation 3.23 can predict all first-order internal multiples and address spurious events by using a new integrand with internal multiples reduced (i.e.,  $b_1(z) + b_3(z)$ )

Equation 3.22 can be easily extended to a multi-dimensional case. In multi-dimensional case, the data comprehensive algorithm can be written as (in comparison with equation 2.13)

$$\mathcal{D}^{IM}(k_g, k_s, \omega) = D(k_g, k_s, \omega) + \mathcal{D}_3(k_g, k_s, \omega), \quad (3.24)$$

Similarly,  $\mathcal{D}_3(k_g, k_s, \omega) = (-2iq_s)^{-1}b_3^{New}(k_g, k_s, \omega)$ , and  $b_3^{New}(k_g, k_s, \omega)$  can be computed directly from

$$\begin{aligned} b_3^{New}(k_g, k_s, \omega) = & \frac{1}{(2\pi)^2} \int_{-\infty}^{\infty} dk_1 \int_{-\infty}^{\infty} dk_2 e^{-iq_1(z_g - z_s)} e^{iq_2(z_g - z_s)} \\ & \times \int_{-\infty}^{\infty} dz_1 [b_1(k_g, k_1, z_1) + b_3(k_g, k_1, z_1)] e^{i(q_g + q_1)z_1} \\ & \times \int_{-\infty}^{z_1 - \epsilon} dz_2 [b_1(k_1, k_2, z_2) + b_3(k_1, k_2, z_2)] e^{-i(q_1 + q_2)z_2} \\ & \times \int_{z_2 + \epsilon}^{\infty} dz_3 [b_1(k_2, k_s, z_3) + b_3(k_2, k_s, z_3)] e^{i(q_2 + q_s)z_3}. \end{aligned} \quad (3.25)$$

In equation 3.25,  $b_1(k_g, k_s, z)$  and  $b_3(k_g, k_s, z)$  has the same meaning as in equation 2.13.

## 4. NUMERICAL TESTS OF THE ISS DATA COMPREHENSIVE INTERNAL MULTIPLE ATTENUATION ALGORITHM

In this chapter, I will apply the extended ISS data-comprehensive internal multiple attenuation algorithm to synthetic data sets to examine and demonstrate the added value from the extended algorithm. The tests are carried out in both 1D normal incident and 2D cases. In 1D normal incident case, I will first use a synthetic data set from a simple four-reflector model to explicitly examine the effectiveness of the extended data comprehensive algorithm to accommodate both primaries and internal multiples as subevents. Then, I proceed to more realistic and complicated cases where synthetic tests are carried out on realistic well-log based data sets. The numerical test results show the significance and added value of including the higher-order ISS terms where there are many reflectors. The 2D test focuses on code implementation of the extended algorithm using a simple three-reflector example in 2D case.

### 4.1 1D normal incident case

In the first test, I use a four-reflector 1D model to generate the synthetic data set. Figure 4.1 shows the model and parameters. Synthetic data set (shown in Figure 4.2a) which consists of primaries and internal multiples is generated by reflectivity method with a ricker wavelet which has a 25 Hz peak frequency. With this synthetic data set as input, two prediction results can be obtained from the current and extended algorithm. Figure 4.2b and 4.2c compares the data ( $D(t)$ ) with the prediction result from the current ( $-D_3(t)$ ) and

extended ( $-\mathcal{D}_3(t)$ ) algorithm, respectively. Notice here, I flip the polarity of the prediction result for easy comparison with the data itself in Figures 4.2b and 4.2c.

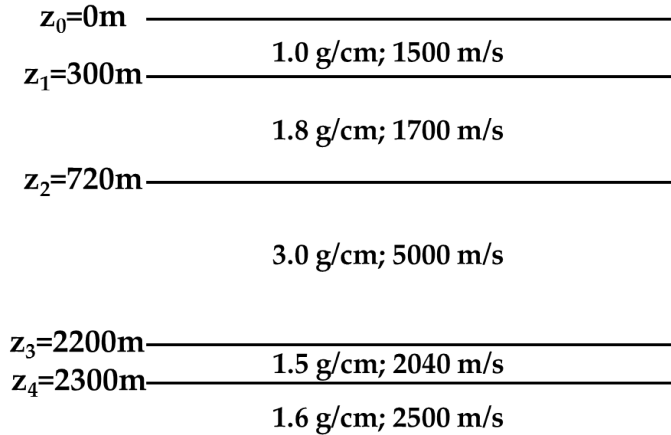
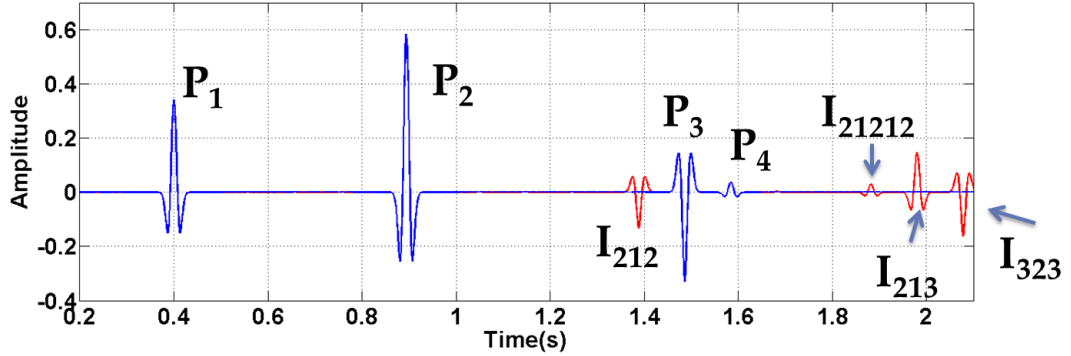


**Fig. 4.1:** A model with four horizontal reflectors to generate synthetic data set.

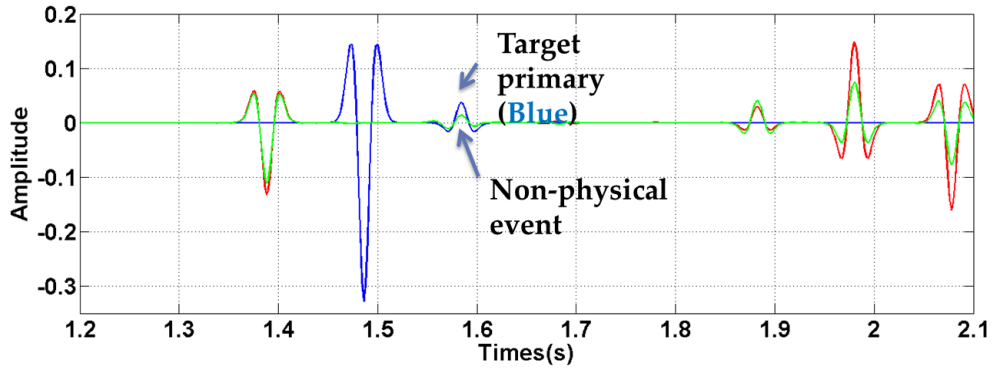
In the next two tests, I will first use information from field well-log data to generate 1D model with parameters (e.g., depth of the reflectors, velocity and density for each layer) closer to real geology. Then, based on the 1D model derived from well-log data, synthetic data sets consisting of primaries and internal multiples are generated using reflectivity method.

Figure 4.3 shows the velocity model derived from the well-log data of Saudi Arabian Oil Co.. Using this velocity model, I use reflectivity method and a ricker wavelet with 25 Hz peak frequency generate synthetic data consist of primaries and internal multiples.

Figure 4.4a and Figure 4.4b shows the comparison between the actual first-order internal multiples in the data and the prediction result from the current and extended algorithm. respectively. Compared with the model shown in Figure 4.1, the model shown in Figure 4.3 contains much more reflectors, therefore, synthetic data set generated by this model will be much more complicated and consists of many events. Furthermore, events are no longer isolated from each other. Hence, it is difficult/impossible to label events with their



**Fig. 4.2a:** Synthetic data set ( $D(t)$ ) generated using model 4.1. There are four primaries ( $P_1, P_2, P_3, P_4$ ) corresponding four reflectors, and four internal multiples ( $I_{212}, I_{21212}, I_{213}, I_{323}$ ). Numbers in the subscript represent the location where reflections happen. For example,  $P_1$  corresponds to the primary with the upward reflection at the first reflector while  $I_{212}$  corresponds to the first-order internal multiple with reflections at the second-first-second reflector. Notice that  $I_{21212}$  is a second-order internal multiple. In the figure, primaries and internal multiples are represented by blue and red, respectively.



**Fig. 4.2b:** Comparison between the data (i.e.,  $D(t)$ , blue for primaries and red for internal multiples) and prediction result (green for prediction) from the current algorithm (i.e.,  $-D_3(t)$ ). The comparison shows that four internal multiples (around 1.4s, 1.9s, 2s, and 2.1s) are predicted with accurate time and approximate amplitude. However, besides the prediction of internal multiples, a non-physical event is produced which happens to interfere with the target primary (around 1.6s). Without knowing the event around 1.6s is a non-physical event, the target primary could be misinterpreted as an internal multiple.

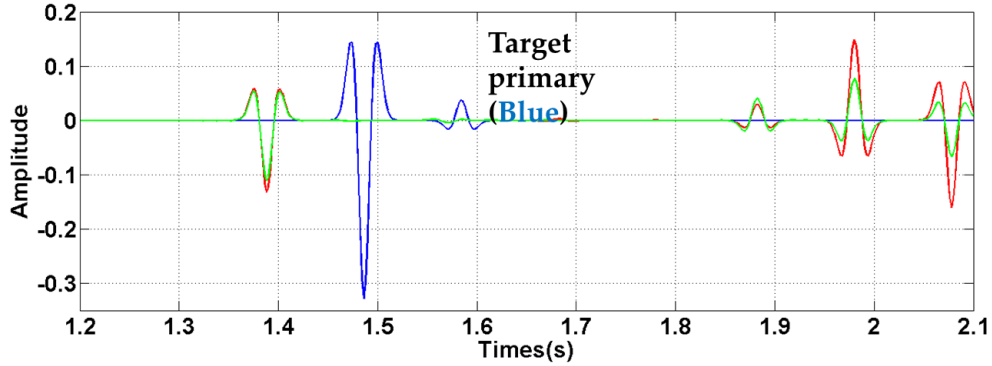


**Fig. 4.2c:** Comparison between the data (i.e.,  $D(t)$ , blue for primaries and red for internal multiples) and prediction result from the extended algorithm (i.e.,  $-\mathcal{D}_3(t)$ , green for prediction). Comparing prediction result from Figure 4.2b and prediction result shown in this figure demonstrates that the extended algorithm retains the effectiveness in predicting internal multiples while addresses non-physical events at the same time.

reflections as in the previous simple four-reflector test. Comparing these two predictions, it is concluded that, the extended algorithm further improves the effectiveness of predicting internal multiples by reducing the spurious events.

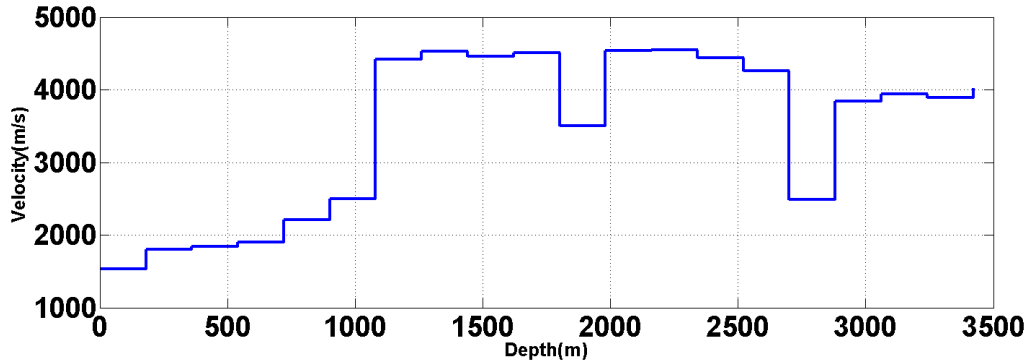


**Fig. 4.3:** Velocity model used to generate synthetic data (courtesy of Saudi Arabian Oil Co.).

A similar test is carried out based on well-log data from Kuwait Oil Company (KOC). Figure 4.5 shows velocity and density variations as a function of depth derived from well-log data from KOC. Compared with the model in the last test, the model in this test contains more reflectors. Hence, the synthetic data generated in this test will be further more complicated. In Figure 4.6a and 4.6a, I provide the comparisons between actual

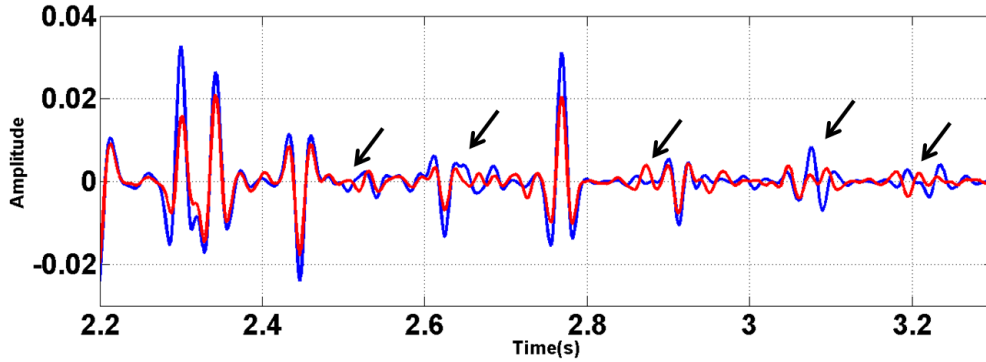


**Fig. 4.4a:** Comparison between the actual first-order internal multiples (in blue) and prediction result (i.e.,  $-D_3(t)$  in red) from the current algorithm. The prediction result from the current algorithm is very close to the actual first-order internal multiples in the data. However, there are several noticeable disagreement between the actual the prediction from the current algorithm highlighted by arrows

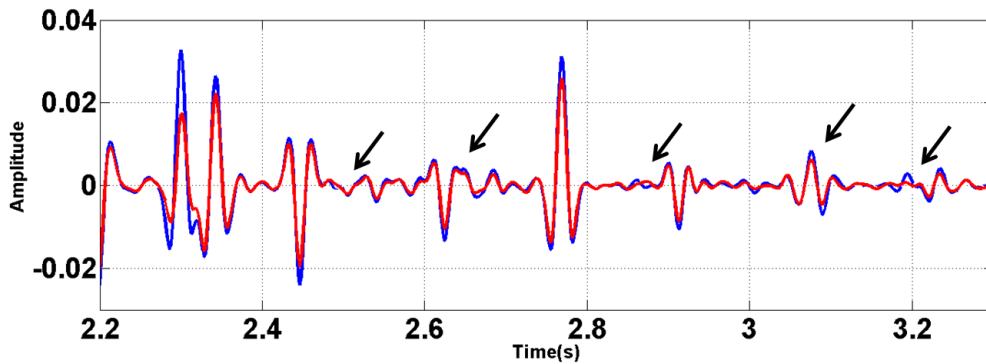


**Fig. 4.4b:** Comparison between the actual first-order internal multiples (in blue) and prediction result (i.e.,  $-D_3(t)$  in red) from the current algorithm. Compared with the prediction result from the current algorithm in Figure 4.4a, this extend algorithm delivers further effectiveness in predicting internal multiples (highlighted by arrows) in the cases where there are many reflectors as analyzed in the last chapter.

internal multiples of all orders in the data and prediction result from the current and extended algorithm, respectively. Similarly, this test further demonstrates the added value in predicting internal multiples accurately with the extended algorithm.

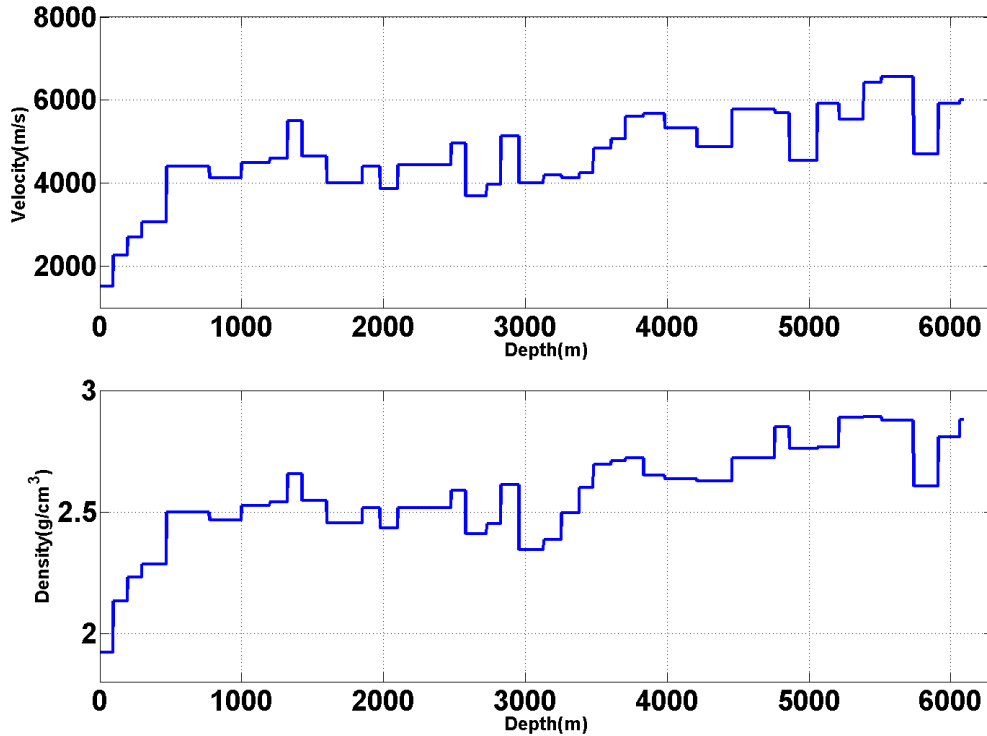


*Fig. 4.5:* Velocity and density blocking from well-log data (courtesy of Kuwait Oil Company).

#### 4.2 2D case

In this section, we test the extended algorithm in 2D case. Figure 4.7 shows the model used to generate synthetic data set consists of primaries and internal multiples with finite difference method. Notice there are three reflectors in this model with a trench in the middle of the model. Parameters in this model are chosen to generate strong internal multiples in the data. For example, normal incident reflection coefficient corresponding to the second reflector is around 0.8, which is very rare in real geological cases. The synthetic data consist

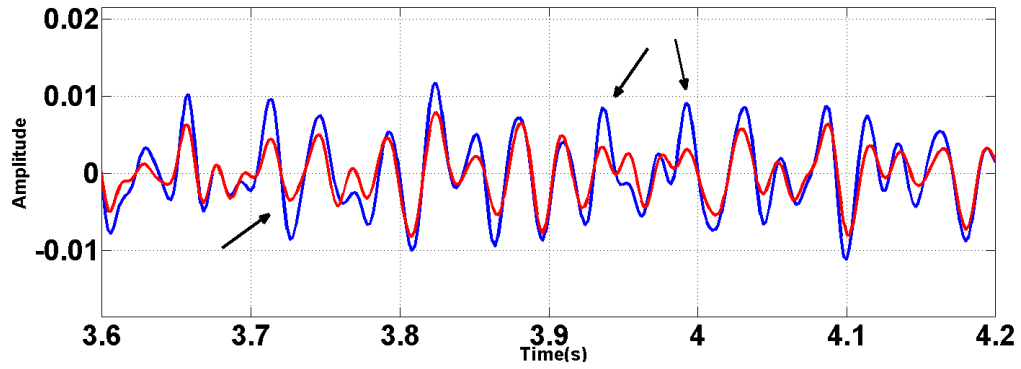


**Fig. 4.6a:** Comparison between actual internal multiples of all orders (in blue) and prediction (i.e.,  $-D_3(t)$  in red) from current algorithm.

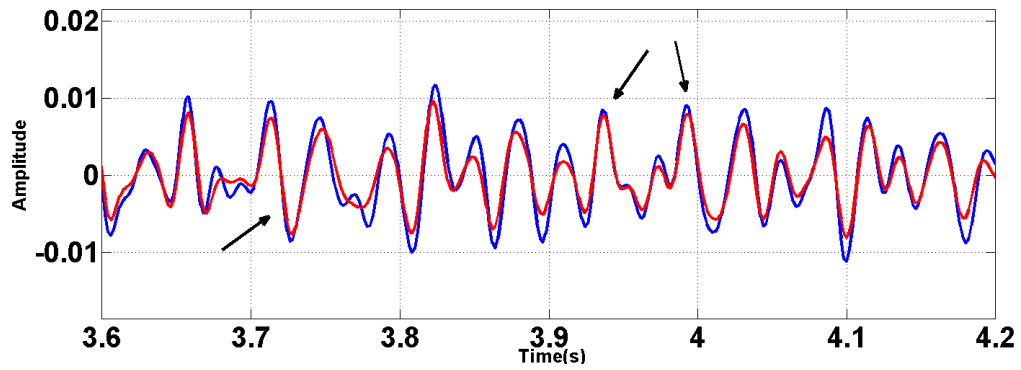


**Fig. 4.6b:** Comparison between actual internal multiples of all orders (in blue) and prediction (i.e.,  $-D_3(t)$  in red) from extended algorithm.

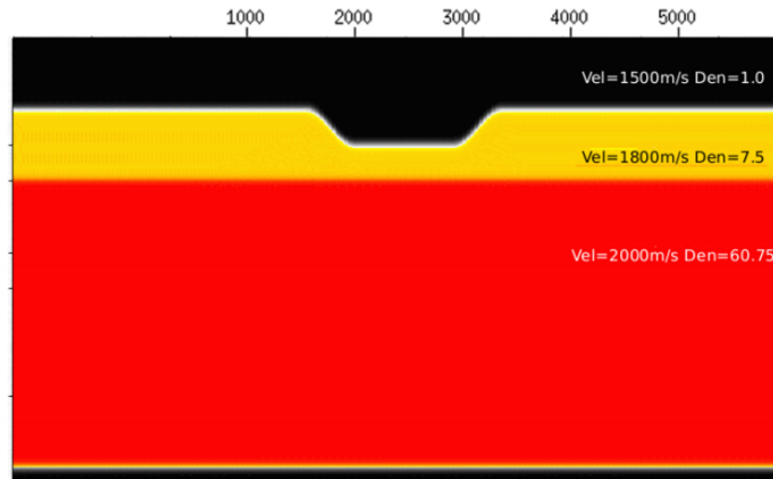


**Fig. 4.7:** Synthetic velocity and density model used to generate the test data in this section (courtesy of WesternGeco). The average dip of the walls of the trench featuring in the center of the model is approximately 20 degree (Figure adapted from Terenghi and Weglein (2011)).

of 251 shots  $\times$  251 receivers, with both shot- and receiver-interval of 25 m, each trace has 501 samples with a total duration 4s.

Figure 4.8a and Figure 4.8b show the several trace comparisons between the actual internal multiples (in red) in the data and prediction results (in blue) from the current and extended algorithm, respectively. The comparisons shown in Figure 4.8 demonstrated in extended algorithm, in 2D case, can provide further effectiveness on prediction internal multiples in the data.

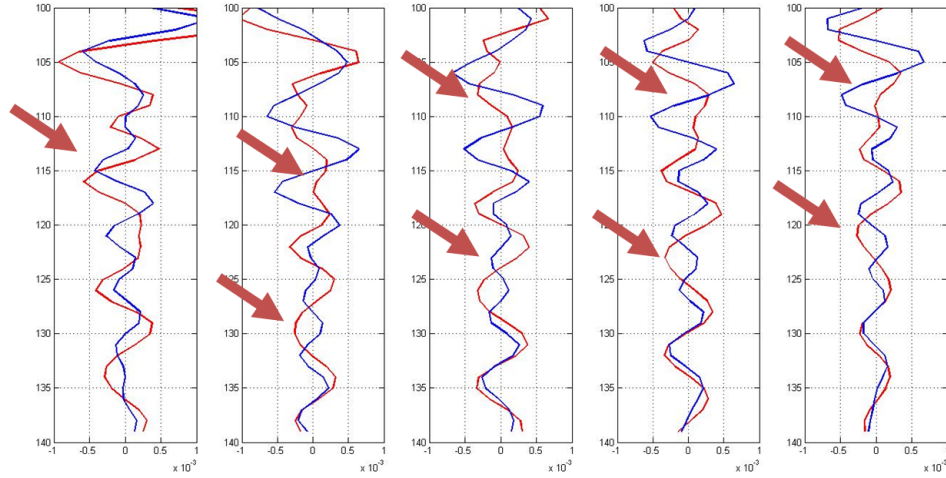


**Fig. 4.8a:** A shot comparison between the test data (left part) and the ISS internal multiple prediction (right part) **without** addressing the spurious events.

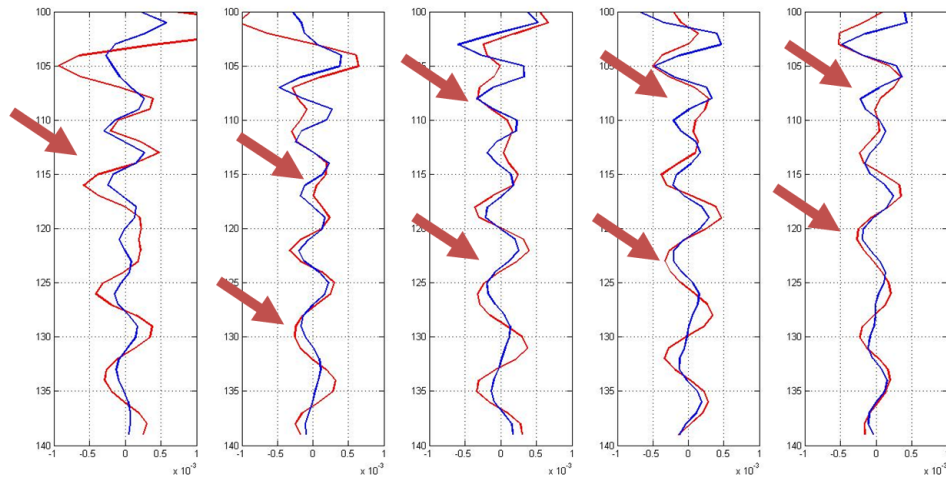


**Fig. 4.8b:** A shot comparison between the test data (left part) and the ISS internal multiple prediction (right part) **with** addressing the spurious events.

## 5. USE OF MULTIPLES TO OBTAIN AN APPROXIMATE IMAGE OF AN UNRECORDED PRIMARIES TO ENHANCE THE SUBSURFACE STRUCTURAL IMAGING

This chapter provides the study of using multiples to enhance subsurface structural imaging when there is an inadequate collection of primaries by obtaining an approximate image of unrecorded primaries.

As described in the Introduction, multiples have more than one upward reflections, and involve the cumulative effect of more than one reflection interactions. The relationship between multiples and earth is more complicated than the relationship between the primaries and earth. The primary-only assumption simplifies the processing of seismic data for determining the spatial locations and mechanical property change. Multiples in that process will result in a false, misleading and potentially injurious subsurface image, and hence multiples need to be predicted and removed from the data. Hence, seismic imaging and inversion algorithms assumes the input data consists of only primaries and removal of multiples is a pre-requisite.

However, whereas imaging requires only primaries, circumstances exist in which the extent, sampling and acquisition of primaries is incomplete and less than adequate to achieve imaging objectives. Researchers (e.g., Berkhout and Verschuur (1994); Shan (2003); Muijs *et al.* (2007); Whitmore *et al.* (2010); Lu *et al.* (2011) and Valenciano *et al.* (2014)) seek- ing methods that use multiples to extract an approximate image of unrecorded primaries were influenced and inspired by the Claerbout imaging condition II (designed for imaging



compute the zero lag of the crosscorrelation of the source and receiver wavefield. This can be expressed by equation 5.2.

$$Map(x, z) = \int U(x, z, \omega) D^*(x, z, \omega) d\omega, \quad (5.2)$$

where  $U(x, z, \omega)$  and  $D(x, z, \omega)$  are Fourier Transform over time of  $U(x, z, t)$  and  $D(x, z, t)$ , respectively. \* means complex conjugate. Equation 5.2 can be expressed in time domain as follows:

$$Map(x, z) = \int U(x, z, t) D(x, z, t) dt. \quad (5.3)$$

Next, an analytic example is provided to illustrate the use of equation 5.2 to locate a

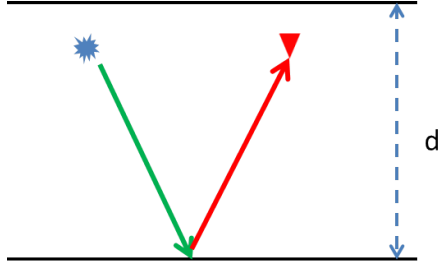


**Fig. 5.2:** Image of a recorded primary.

reflector. Consider a 1D normal incident plane wave that starts at  $\epsilon_s$  at  $t = 0$ , the plane wave travels down from the source to the reflector at depth  $d$ , and hits the reflector and travels upward to the receiver at  $\epsilon_g$  (Figure 5.2). In this simple experiment, the  $D$  and  $U$  waves are

$$D(z, \omega) = e^{i\omega[\frac{z-\epsilon_s}{c_0}]}, \quad (5.4)$$

$$U(z, \omega) = R_1 e^{i\omega[\frac{d-\epsilon_s}{c_0} + \frac{d-z}{c_0}]}, \quad (5.5)$$

respectively, where  $R_1$  is the reflection coefficient,  $c_1$  is the velocity.

With equations 5.4 and 5.5, equation 5.2 produces

$$\begin{aligned}
 Map(x, z) &= \int U(x, z, \omega) D^*(x, z, \omega) d\omega \\
 &= \int (R_1 e^{i\omega[\frac{d-\epsilon_s}{c_0} + \frac{d-z}{c_0}]}) (e^{-i\omega[\frac{z-\epsilon_s}{c_0}]}) d\omega \\
 &= \int R_1 e^{i\omega[\frac{2d-2z}{c_0}]} d\omega \\
 &= \frac{c_0}{2} R_1 \delta(d - z).
 \end{aligned} \tag{5.6}$$

That is, equation 5.2 correctly locate the reflector at depth  $d$ .

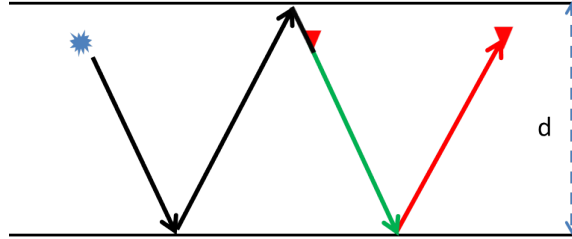


**Fig. 5.3:** Image of an unrecorded primary.

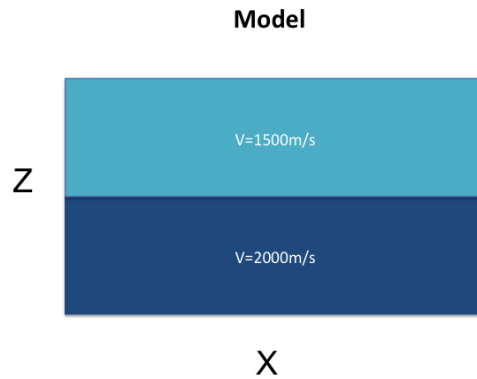
For the purpose of using a multiple to find an approximate image of an unrecorded primary, we consider the field  $U$  (in equation 5.2) as the source-and-receiver deghosted first-order multiple (represented by the black-green-red line in Figure 5.3),  $-R_1^2 e^{i\omega[\frac{d-\epsilon_s}{c_0} + \frac{2d}{c_0} + \frac{d-z}{c_0}]}$ , and the field  $D$  as the source-deghosted, but the receiver ghost of the primary (represented by the black line in Figure 5.3) that is a subevent of a recorded multiple,  $-R_1 e^{i\omega[\frac{d-\epsilon_s}{c_0} + \frac{d+z}{c_0}]}$ . That interpretation of equation 5.2, with that input  $D$  and  $U$ , will produce an appropriate

image of the unrecorded subevent of the multiple,

$$\begin{aligned}
 Map(x, z) &= \int U(x, z, \omega) D^*(x, z, \omega) d\omega \\
 &= \int (-R_1^2 e^{i\omega[\frac{d-\epsilon_s}{c_0} + \frac{2d}{c_0} + \frac{d-z}{c_0}]}) (-R_1 e^{-i\omega[\frac{d-\epsilon_s}{c_0} + \frac{d+z}{c_0}]}) d\omega \\
 &= \int R_1^3 e^{i\omega[\frac{2d-2z}{c_0}]} d\omega \\
 &= \frac{c_0}{2} R_1^3 \delta(d - z).
 \end{aligned} \tag{5.7}$$

Within that understanding, we use a 1D prestack example to examine the imaging result of an unrecorded primary that we can extract from multiples following Claerbout's imaging condition II. I provide a 1D prestack numerical example, based on a one horizontal reflector model, to examine the result of approximately imaging an unrecorded primary extracted from a recorded multiple. The image results are obtained by the following equation:

$$Map(x, z) = \int U(x, z, t) D(x, z, t) dt. \tag{5.8}$$



**Fig. 5.4:** A test model for a case of a single horizontal reflector.

The test data are generated from a model that contains one horizontal reflector (Figure 5.4). In imaging the recorded primary (Figure 5.5), the downgoing wavefield that is being forward propagated is the source wavefield, and the upgoing wavefield that is being backward propagated is the primary. In imaging the unrecorded primary (Figure 5.5), the downgoing wavefield that is being forward propagated is the receiver-side ghost of the primary, and the upgoing wavefield that is being backward propagated is the source-receiver-side-deghosted first-order free-surface multiple.

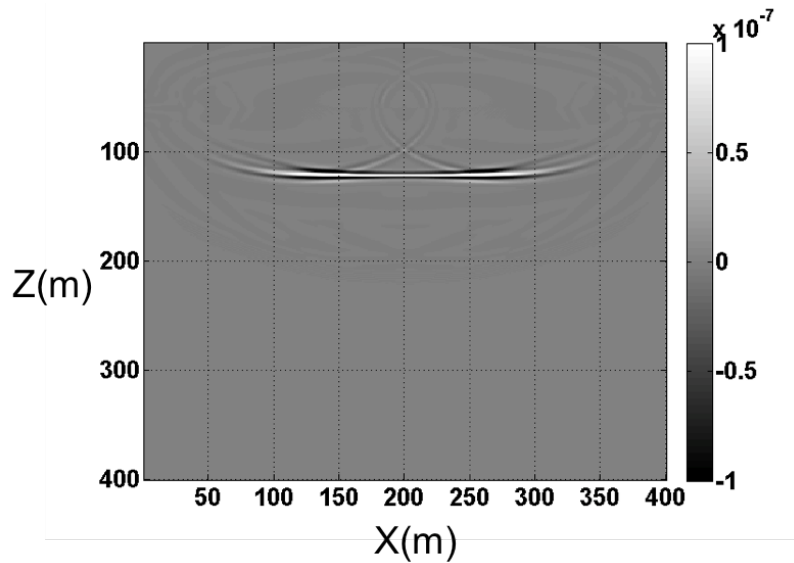


**Fig. 5.5:** result from imaging a primary following Claerbout's imaging condition II.

Comparing the result in Figure 5.5 with the result in Figure 5.6, we note that the reflector is correctly imaged in both results. However, the image from the unrecorded primary (extracted from a multiple) shows broader illumination (with smaller image amplitude) compared with the image from the recorded primary.

It is important to point out that in obtaining the result of Figure 5.6 in this synthetic example, we purposefully chose the receiver-side ghost of the primary and the source-receiver-side-deghosted first-order free-surface multiple as the down-going ( $D$ ) and up-going ( $U$ ) wavefields, respectively. Methods that seek to obtain an approximate image of an un-

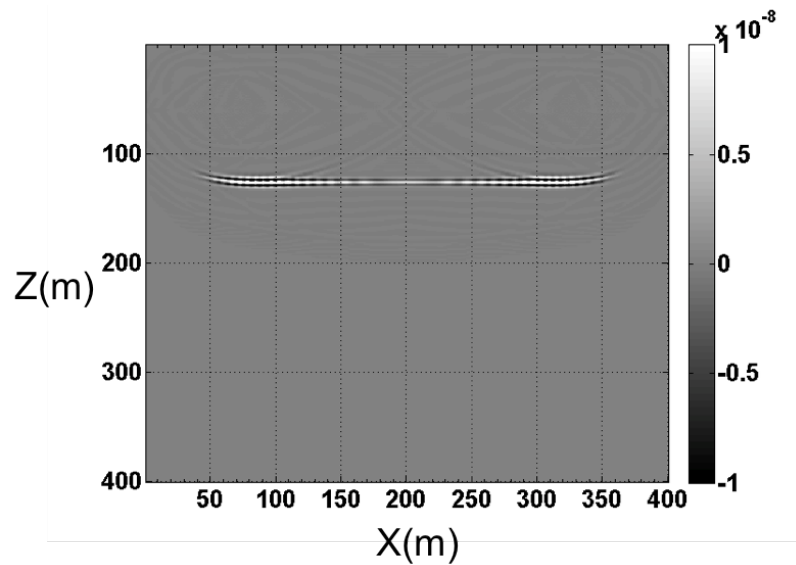


**Fig. 5.6:** result from imaging an extracted primary from a first-order free-surface multiple following Claerbout's imaging condition II.

recorded primary require an effective up-down wavefield separation, which can be achieved by modern seismic acquisition techniques (e.g., GeoStreamer or over/under cable). Notice that, among different combinations between the downgoing and upgoing events, cross-talk artifacts can happen (e.g., Lu *et al.* (2011)).

## 6. SUMMARY

The current ISS internal multiple attenuation algorithm has shown differential added-value, in comparison with other internal multiple suppression methods for complex exploration areas where internal multiple generators are difficult to be identified. This algorithm has been recognized as the most capable internal multiple suppression method by the petroleum industry.

The ISS internal multiple attenuation algorithm consists of the ISS internal multiple attenuators of different orders. Each internal multiple attenuator of given order uses primaries in the input data to predict internal multiples of that order from all reflectors at once with accurate time and approximate amplitude and without subsurface information. However, the input data consist of both primaries and internal multiples. This dissertation shows when the internal multiples in the input data enter the ISS attenuator of a given order, they (1) contributes to higher-order internal multiple removal and (2) under certain circumstances can cause false or spurious events. Terms in the internal multiple removal subseries, which are of higher order than the ISS internal multiple attenuator, have the purpose and capability of addressing a shortcoming of its lower order and less accommodating relative.

The new internal multiple algorithm within this dissertation combines the original lower order attenuation algorithm with the inclusion and assist of the higher order terms, providing a comprehensive internal multiple attenuator that can accommodate primaries and internal multiples in the input data. That new higher-order algorithm provides all the benefit of the original ISS internal multiple attenuation algorithms without its deficits and shortcomings.

This first part of this dissertation contributes to identifying those higher-order terms, and examining, testing and analyzing the relevant and practical benefit provided by this higher-order algorithm. Synthetic tests demonstrated this higher-order algorithm retains the same effectiveness of the original algorithm and now can accommodate both primaries and internal multiples as input. This dissertation is also part of an overall strategy to use the ISS to provide further capability for internal multiple prediction and removal in extremely complicated onshore and offshore exploration cases.

In principle, only primaries are called for to determine structure and to identify subsurface properties. Multiples, along with reference wave, ghosts, need to be predicted and removed from the seismic data in order to obtain the primary-only input to the imaging and inversion methods. However, when the collection of primaries is incomplete and less than adequate, then the predicted multiples can, at times, be used to provide an approximate image of unrecorded primaries. The latter can supplement the subsurface structural image from recorded primaries. The second part of this dissertation studies the procedure of using multiples to provide an approximate image of unrecorded primaries. A numerical example illustrates the added-value from that procedure.

In summary, this dissertation contributes to two important topics in exploration seismology, (1) identifying and removing multiples and (2) using multiples. This dissertation shows multiples can be used to provide an approximate image of unrecorded primaries to enhance the subsurface structural from recorded primaries. However, multiples need to be first predicted and removed from the data before imaging the recorded primaries for processing goals that seek to effectively locate and invert reflections. The removal of multiples remains a key open issue, and high priority pressing challenge. This dissertation is part of an overall strategy to use the ISS to provide further capability for internal multiple prediction and removal in extremely complicated onshore and complex offshore exploration cases.

## REFERENCES

- ARAÚJO, F. V. 1994. Linear and non-linear methods derived from scattering theory: backscattered tomography and internal multiple attenuation. Ph.D. thesis, Universidade Federal da Bahia.
- ARAÚJO, F. V., WEGLEIN, A. B., CARVALHO, P. M., AND STOLT, R. H. 1994. Inverse scattering series for multiple attenuation: An example with surface and internal multiples. *SEG Technical Program Expanded Abstracts*, 1039–1041.
- BAYSAL, E., KOSLOFF, D. D., AND SHERWOOD, J. W. C. 1983. Reverse time migration. *Geophysics* 48, 1514–1524.
- BERKHOUT, A. J. AND VERSCHUUR, D. J. 1994. Multiple technology: Part 2, migration of multiple reflections. *SEG Technical Program Expanded Abstracts*, 1497–1500.
- CARVALHO, P. M. 1992. Free-surface multiple reflection elimination method based on nonlinear inversion of seismic data. Ph.D. thesis, Universidade Federal da Bahia.
- CARVALHO, P. M., WEGLEIN, A. B., AND STOLT, R. H. 1991. Examples of a nonlinear inversion method based on the T-matrix of scattering theory: Application to multiple suppression. In *61st Ann. Internat. Mtg. Soc. of Expl. Geophys., Expanded Abstracts*. Soc. Expl. Geophys., 1319–1322.
- CLAERBOUT, J. F. 1971. Toward a unified theory of reflector mapping. *Geophysics* 36, 3, 467–481.

- DESANTO, J. A. 1992. *Scalar Wave Theory: Green's Functions and Applications*. Springer-Verlag.
- FERREIRA, A. 2011. Internal multiple removal in offshore brazil seismic data using the inverse scattering series. Ph.D. thesis, University of Houston.
- FU, Q., LUO, Y., KELAMIS, P. G., HUO, S., SINDI, G., HSU, S.-Y., AND WEGLEIN, A. 2010. The inverse scattering series approach towards the elimination of land internal multiples. *SEG Technical Program Expanded Abstracts 29*, 3456–3461.
- HSU, S., TERENCEHI, P., AND WEGLEIN, A. B. 2010. The properties of the inverse scattering series internal multiple attenuation algorithm: Analysis and evaluation on synthetic data with lateral variations, choosing reference velocity and examining its sensitivity to near surface properties. *Mission-Oriented Seismic Research Program (M-OSRP) Annual Report*, 1628.
- INNANEN, K. A. AND WEGLEIN, A. B. 2003. Simultaneous imaging and inversion with the inverse scattering series. In *Proceedings of the Eighth International Congress of the SBGf and Fifth Latin American Geophysical Conference*. SBGf.
- KELAMIS, P. G., LUO, Y., AND WEGLEIN, A. 2013. Strategies of land internal multiple elimination based on inverse scattering series. *Presented at the 6th International Petroleum Technology Conference*.
- LIANG, H., MA, C., AND WEGLEIN, A. 2013. General theory for accommodating primaries and multiples in internal multiple algorithm: Analysis and numerical tests. *SEG Technical Program Expanded Abstracts*, 4178–4183.
- LIU, F. AND WEGLEIN, A. 2014. The first wave equation migration rtm with data consisting of primaries and internal multiples: theory and 1d examples. *Journal of Seismic Exploration 23*, 357–366.

## References

---

- LU, S., WHITEMORE, N., VALENCIANO, A., AND CHEMINGUI, N. 2011. Imaging of primaries and multiples with 3d seam synthetic. *SEG Technical Program Expanded Abstracts*, 3217–3221.
- LUO, Y., G.KELAMIS, P., FU, Q., HUO, S., SINDI, G., HSU, S.-Y., AND WEGLEIN, A. 2011. Elimination of land internal multiples based on the inverse scattering series. *The Leading Edge* 30, 884–889.
- MA, C., LIANG, H., AND WEGLEIN, A. 2011. Modifying the leading order iss attenuator of first-order internal multiples to accommodate primaries and internal multiples: fundamental concept and theory, development, and examples exemplified when three reflectors generate the data. *Mission-Oriented Seismic Research Program (M-OSRP) 2011 Annual Report*, 133–147.
- MATSON, K., CORRIGAN, D., WEGLEIN, A., YONG, C. Y., AND CARVALHO, P. 1999. Inverse scattering internal multiple attenuation: Results from complex synthetic and field data examples. *SEG Expaned Abstract*.
- MATSON, K. H. 1997. An inverse-scattering series method for attenuating elastic multiples from multicomponent land and ocean bottom seismic data. Ph.D. thesis, University of British Columbia.
- MATSON, K. H. AND WEGLEIN, A. B. 1996. The relationship between scattering theory and the primaries and multiples of reflection seismic data. *Journal of Seismic Exploration* 5, 63–78.
- MCMECHAN, G. A. 1983. Migration by extrapolation of time-dependent boundary values. *Geophysical prospecting* 31, 413–420.
- MOSES, H. 1956. Calculation of scattering potential from reflection coefficients. *Phys. Rev.* 102, 559–567.

- MUIJS, R., ROBERTSSON, J. O. A., AND HOLLIGER, K. 2007. Prestack depth migration of primary and surface-related multiple reflections: Part i imaging. *Geophysics*, S59–S69.
- NITA, B. G. AND WEGLEIN, A. B. 2007. Inverse scattering internal multiple attenuation algorithm: An analysis of the pseudo-depth and time-monotonicity requirements. *SEG Technical Program Expanded Abstracts*, 2461–2465.
- PROSSER, R. T. 1969. Formal solutions of inverse scattering problems. *Journal of Mathematical Physics* 10, 10, 1819–1822.
- RAMIREZ, A. 2007. I-inverse scattering subseries for removal of internal multiples and depth imaging primaries;ii-green’s theorem as the foundation of interferometry and guiding new practical methods and applications. Ph.D. thesis, University of Houston.
- RAZAVY, M. 1975. Determination of the wave velocity in an inhomogeneous medium from reflection data. *J. Acoust. Soc. Am.* 58, 956–963.
- SHAN, G. 2003. Source-receiver migration of multiple reflections. *SEG Technical Program Expanded Abstracts*, 1008–1011.
- SHAW, S. A. 2005. An inverse scattering series algorithm for depth imaging of reflection data from a layered acoustic medium with an unknown velocity model. Ph.D. thesis, University of Houston.
- STOLT, R. H. AND JACOBS, B. 1980. Inversion of seismic data in a laterally heterogeneous medium. *Stanford Exploration Project* 24.
- TAYLOR, J. R. 1972. *Scattering theory: the quantum theory of nonrelativistic collisions*. John Wiley & Sons, Inc.
- TERENGI, P., HSU, S.-Y., B.WEGLEIN, A., AND LI, X. 2011. Exemplifying the specific properties of the inverse scattering series internal-multiple attenuation method that reside behind its capability for complex onshore and marine multiples. *The Leading Edge*.

- TERENGI, P. AND WEGLEIN, A. B. 2011. Iss internal multiple attenuation with angle constraints. *Mission-Oriented Seismic Research Program (M-OSRP) Annual Report*, 242–266.
- VALENCIANO, A. A., CRAWLEY, S., KLOCHIKHINA, E., CHEMINGUI, N., LU, S., AND WHITEMORE, D. 2014. Imaging complex structures with separated up- and down-going wavefields. *SEG Technical Program Expanded Abstracts*, 3941–3945.
- WEGLEIN, A. AND DRAGOSET, W. 2005. *Multiple Attenuation*. Geophysics reprint series. Soc. Expl. Geophys.
- WEGLEIN, A., HSU, S.-Y., TERENGI, P., LI, X., AND STOLT, R. H. 2011. Multiple attenuation: Recent advances and the road ahead (2011). *The Leading Edge*, 864–875.
- WEGLEIN, A., STOLT, R. H., AND MAYHAN, J. D. 2011a. Reverse-time migration and greens theorem: Part i the evolution of concepts, and setting the stage for the new rtm method. *Journal of Seismic Exploration* 20, 73–90.
- WEGLEIN, A., STOLT, R. H., AND MAYHAN, J. D. 2011b. Reverse-time migration and greens theorem: Part ii a new and consistent theory that progresses and corrects current rtm concepts and methods. *Journal of Seismic Exploration* 20, 135–159.
- WEGLEIN, A. B. 2013. The multiple attenuation toolbox: Progress, challenges and open issues. *SEG Technical Program Expanded Abstracts*, 4493–4499.
- WEGLEIN, A. B. 2016. Multiple:signal or noise? *Geophysics* 81, 4, v283–v302.
- WEGLEIN, A. B., ARAÚJO, F. V., CARVALHO, P. M., STOLT, R. H., MATSON, K. H., COATES, R. T., CORRIGAN, D., FOSTER, D. J., SHAW, S. A., AND ZHANG, H. 2003. Inverse scattering series and seismic exploration. *Inverse Problems* 19, R27–R83.

## References

---

- WEGLEIN, A. B., BOYCE, W. E., AND ANDERSON, J. E. 1981. Obtaining three-dimensional velocity information directly from reflection seismic data: An inverse scattering formalism. *Geophysics* 46, 8, 1116–1120.
- WEGLEIN, A. B., GASPAROTTO, F. A., CARVALHO, P. M., AND STOLT, R. H. 1997. An inverse-scattering series method for attenuating multiples in seismic reflection data. *Geophysics* 62, 6 (November-December), 1975–1989.
- WEGLEIN, A. B. AND MATSON, K. H. 1998. Inverse scattering internal multiple attenuation: An analytic example and subevent interpretation. In *SPIE Conference on Mathematical Methods in Geophysical Imaging*. 108–117.
- WEGLEIN, A. B. AND SECREST, B. G. 1990. Wavelet estimation for a multidimensional acoustic earth model. *Geophysics* 55, 7 (July), 902–913.
- WHITMORE, N. D. 1983. Iterative depth migration by backward time propagation. *SEG Technical Program Expanded Abstracts*, 382–385.
- WHITMORE, N. D., VALENCIANO, A., SLLNER, W., AND LU, S. 2010. Imaging of primaries and multiples using adual-sensor towed streamer. *SEG Technical Program Expanded Abstracts*, 3187–3192.
- ZHANG, H. AND SHAW, S. 2010. 1-d analytical analysis of higher order internal multiples predicted via the inverse scattering series based algorithm. *SEG Expanded Abstracts* 29, 3493–3498.

## APPENDICES

## A. DERIVATION OF EQUATION 3.20

One portion of the fifth order term in the ISS is capable of predicting the artifacts we want to remove. Start from the fifth order equation,

$$\begin{aligned}
 V_5 = & -V_1G_0V_1G_0V_1G_0V_1G_0V_1 - V_2G_0V_1G_0V_1G_0V_1 - V_1G_0V_2G_0V_1G_0V_1 \quad (\text{A.1}) \\
 & -V_1G_0V_1G_0V_2G_0V_1 - V_1G_0V_1G_0V_1G_0V_2 - V_3G_0V_1G_0V_1 \\
 & -V_1G_0V_3G_0V_1 - V_1G_0V_1G_0V_3 - V_4G_0V_1 - V_1G_0V_4
 \end{aligned}$$

Inspired by the analog between the forward and inverse series and the logic of constructing internal multiple using primaries,  $V_{57} = V_1G_0V_3G_0V_1$  is chosen for further study. Using effective data in the pseudo-depth domain to express it as (Ramirez, 2007),

$$\begin{aligned}
 B_{57}(k) = & \int_{-\infty}^{\infty} dz b_1(z) \int_{-\infty}^{\infty} dz' \hat{b}_3(z') \int_{-\infty}^{\infty} dz'' e^{ikz''} b_1(z'') \quad (\text{A.2}) \\
 & + \int_{-\infty}^{\infty} dz b_1(z) \int_{-\infty}^{\infty} dz' e^{-ikz'} \hat{b}_3(z') \int_{-\infty}^{\infty} dz'' b_1(z'') \\
 & + \int_{-\infty}^{\infty} dz e^{ikz} b_1(z) \int_{-\infty}^{\infty} dz' e^{-ikz'} \hat{b}_3(z') \int_{-\infty}^{\infty} dz'' e^{ikz''} b_1(z'') \\
 & + \int_{-\infty}^{\infty} dz e^{ikz} b_1(z) \int_{-\infty}^{\infty} dz' \hat{b}_3(z') \int_{-\infty}^{\infty} dz'' b_1(z'')
 \end{aligned}$$

where  $\hat{b}_3(z')$  is the data representation of one portion of third order terms such that  $\hat{b}_3(z')$  can be employed to predicted the artifacts.

To make sure the prediction of the correct time, the third term is chosen, and in order to satisfy the "lower-higher-lower" requirement in the pseudo-depth domain, the rightmost

and middle integral limits are further separated as follows,

$$\begin{aligned}
 B_{573}(k) &= \int_{-\infty}^{\infty} dz e^{ikz} b_1(z) \int_{-\infty}^{\infty} dz' e^{-ikz'} \hat{b}_3(z') \int_{-\infty}^{\infty} dz'' e^{ikz''} b_1(z'') \quad (\text{A.3}) \\
 &= \int_{-\infty}^{\infty} dz e^{ikz} b_1(z) \left( \int_{-\infty}^{z-\epsilon} + \int_{z-\epsilon}^{z+\epsilon} + \int_{z+\epsilon}^{\infty} \right) dz' e^{-ikz'} \hat{b}_3(z') \\
 &\quad \times \left( \int_{-\infty}^{z'-\epsilon} + \int_{z'-\epsilon}^{z'+\epsilon} + \int_{z'+\epsilon}^{\infty} \right) dz'' e^{ikz''} b_1(z'') \\
 &= \int_{-\infty}^{\infty} dz e^{ikz} b_1(z) \int_{-\infty}^{z-\epsilon} dz' e^{-ikz'} \hat{b}_3(z') \int_{-\infty}^{z'-\epsilon} dz'' e^{ikz''} b_1(z'') \\
 &\quad + \int_{-\infty}^{\infty} dz e^{ikz} b_1(z) \int_{-\infty}^{z-\epsilon} dz' e^{-ikz'} \hat{b}_3(z') \int_{z'-\epsilon}^{z'+\epsilon} dz'' e^{ikz''} b_1(z'') \\
 &\quad + \int_{-\infty}^{\infty} dz e^{ikz} b_1(z) \int_{-\infty}^{z-\epsilon} dz' e^{-ikz'} \hat{b}_3(z') \int_{z'+\epsilon}^{\infty} dz'' e^{ikz''} b_1(z'') \\
 &\quad + \int_{-\infty}^{\infty} dz e^{ikz} b_1(z) \int_{z-\epsilon}^{z+\epsilon} dz' e^{-ikz'} \hat{b}_3(z') \int_{-\infty}^{z'-\epsilon} dz'' e^{ikz''} b_1(z'') \\
 &\quad + \int_{-\infty}^{\infty} dz e^{ikz} b_1(z) \int_{z-\epsilon}^{z+\epsilon} dz' e^{-ikz'} \hat{b}_3(z') \int_{z'-\epsilon}^{z'+\epsilon} dz'' e^{ikz''} b_1(z'') \\
 &\quad + \int_{-\infty}^{\infty} dz e^{ikz} b_1(z) \int_{z-\epsilon}^{z+\epsilon} dz' e^{-ikz'} \hat{b}_3(z') \int_{z'+\epsilon}^{\infty} dz'' e^{ikz''} b_1(z'') \\
 &\quad + \int_{-\infty}^{\infty} dz e^{ikz} b_1(z) \int_{z+\epsilon}^{\infty} dz' e^{-ikz'} \hat{b}_3(z') \int_{-\infty}^{z'-\epsilon} dz'' e^{ikz''} b_1(z'') \\
 &\quad + \int_{-\infty}^{\infty} dz e^{ikz} b_1(z) \int_{z+\epsilon}^{\infty} dz' e^{-ikz'} \hat{b}_3(z') \int_{z'-\epsilon}^{z'+\epsilon} dz'' e^{ikz''} b_1(z'') \\
 &\quad + \int_{-\infty}^{\infty} dz e^{ikz} b_1(z) \int_{z+\epsilon}^{\infty} dz' e^{-ikz'} \hat{b}_3(z') \int_{z'+\epsilon}^{\infty} dz'' e^{ikz''} b_1(z'')
 \end{aligned}$$

From the above separation, we choose the third term since it satisfies the requirement in the pseudo-depth domain. Then we examine the third order term to determine  $\hat{b}_3(z')$ ;

$$V_3 = -V_1 G_1 V_1 G_0 V_1 - V_2 G_0 V_1 - V_1 G_0 V_2. \quad (\text{A.4})$$

For the same reason,  $V_1 G_1 V_1 G_0 V_1$  is chosen to further study. Expressing this term using

effective data and doing the separation,

$$\begin{aligned}
 B_3(k) &= \int_{-\infty}^{\infty} dz e^{ikz} b_1(z) \int_{-\infty}^{\infty} dz' e^{-ikz'} b_1(z') \int_{-\infty}^{\infty} dz'' e^{ikz''} b_1(z'') \quad (\text{A.5}) \\
 &= \int_{-\infty}^{\infty} dz e^{ikz} b_1(z) \left( \int_{-\infty}^{z-\epsilon} + \int_{z-\epsilon}^{z+\epsilon} + \int_{z+\epsilon}^{\infty} \right) dz' e^{-ikz'} b_1(z') \\
 &\quad \times \left( \int_{-\infty}^{z'-\epsilon} + \int_{z'-\epsilon}^{z'+\epsilon} + \int_{z'+\epsilon}^{\infty} \right) dz'' e^{ikz''} b_1(z'') \\
 &= \int_{-\infty}^{\infty} dz e^{ikz} b_1(z) \int_{-\infty}^{z-\epsilon} dz' e^{-ikz'} b_1(z') \int_{-\infty}^{z'-\epsilon} dz'' e^{ikz''} b_1(z'') \\
 &\quad + \int_{-\infty}^{\infty} dz e^{ikz} b_1(z) \int_{-\infty}^{z-\epsilon} dz' e^{-ikz'} b_1(z') \int_{z'-\epsilon}^{z'+\epsilon} dz'' e^{ikz''} b_1(z'') \\
 &\quad + \int_{-\infty}^{\infty} dz e^{ikz} b_1(z) \int_{-\infty}^{z-\epsilon} dz' e^{-ikz'} b_1(z') \int_{z'+\epsilon}^{\infty} dz'' e^{ikz''} b_1(z'') \\
 &\quad + \int_{-\infty}^{\infty} dz e^{ikz} b_1(z) \int_{z-\epsilon}^{z+\epsilon} dz' e^{-ikz'} b_1(z') \int_{-\infty}^{z'-\epsilon} dz'' e^{ikz''} b_1(z'') \\
 &\quad + \int_{-\infty}^{\infty} dz e^{ikz} b_1(z) \int_{z-\epsilon}^{z+\epsilon} dz' e^{-ikz'} b_1(z') \int_{z'-\epsilon}^{z'+\epsilon} dz'' e^{ikz''} b_1(z'') \\
 &\quad + \int_{-\infty}^{\infty} dz e^{ikz} b_1(z) \int_{z-\epsilon}^{z+\epsilon} dz' e^{-ikz'} b_1(z') \int_{z'+\epsilon}^{\infty} dz'' e^{ikz''} b_1(z'') \\
 &\quad + \int_{-\infty}^{\infty} dz e^{ikz} b_1(z) \int_{z+\epsilon}^{\infty} dz' e^{-ikz'} b_1(z') \int_{-\infty}^{z'-\epsilon} dz'' e^{ikz''} b_1(z'') \\
 &\quad + \int_{-\infty}^{\infty} dz e^{ikz} b_1(z) \int_{z+\epsilon}^{\infty} dz' e^{-ikz'} b_1(z') \int_{z'-\epsilon}^{z'+\epsilon} dz'' e^{ikz''} b_1(z'') \\
 &\quad + \int_{-\infty}^{\infty} dz e^{ikz} b_1(z) \int_{z+\epsilon}^{\infty} dz' e^{-ikz'} b_1(z') \int_{z'+\epsilon}^{\infty} dz'' e^{ikz''} b_1(z'')
 \end{aligned}$$

The term we need from the above result is essentially the attenuator, since what we need in  $\hat{b}_3(z')$  is the predicted internal multiple. Notice here the work is almost the same as the work deriving the leading order internal multiple eliminator (Ramirez, 2007); the difference is it needs data self-interaction in Ramirez (2007) while our solution needs *W-like* interaction.

To summarize we have,

$$b_5^{PIP} = B_{5733}(k) = \int_{-\infty}^{\infty} dz e^{ikz} b_1(z) \int_{-\infty}^{z-\epsilon} dz' e^{-ikz'} \hat{b}_3(z') \int_{z'+\epsilon}^{\infty} dz'' e^{ikz''} b_1(z'')$$

where

$$\hat{b}_3(k) = \int_{-\infty}^{\infty} dz e^{ikz} b_1(z) \int_{-\infty}^{z-\epsilon} dz' e^{-ikz'} b_1(z') \int_{z+\epsilon}^{\infty} dz'' e^{ikz''} b_1(z'') \quad (\text{A.6})$$

## B. TYPE I AND TYPE II EQUATIONS IN INVERSE SCATTERING SERIES

In Ma *et al.* (2011), we stated that the higher-order terms addressing spurious prediction can be derived from a portion of a fifth-order term in the inverse series; see equation A.1. In this appendix, we give an argument on why other portions of the fifth-order term cannot be employed for that purpose.

$$\begin{aligned}
 (G_0^d V_5' G_0^d)_m &= - (G_0^d V_1' G_0^d V_1' G_0^d V_1' G_0^d V_1' G_0^d V_1' G_0^d)_m - (G_0^d V_2' G_0^d V_1' G_0^d V_1' G_0^d V_1' G_0^d)_m \quad (\text{B.1}) \\
 &\quad - (G_0^d V_1' G_0^d V_2' G_0^d V_1' G_0^d V_1' G_0^d)_m - (G_0^d V_1' G_0^d V_1' G_0^d V_2' G_0^d V_1' G_0^d)_m \\
 &\quad - (G_0^d V_1' G_0^d V_1' G_0^d V_1' G_0^d V_2' G_0^d)_m - (G_0^d V_1' G_0^d V_3' G_0^d V_1' G_0^d)_m - (G_0^d V_1' G_0^d V_1' G_0^d V_3' G_0^d)_m \\
 &\quad - (G_0^d V_4' G_0^d V_1' G_0^d)_m - (G_0^d V_1' G_0^d V_4' G_0^d)_m.
 \end{aligned}$$

First, we show that there are differences between different terms in equation B.1; i.e., there exists no reduction in type II terms. To prove that, we first review the reduction case in type I terms.

- Type I

- Begin with equation (11') in Weglein *et al.* (2003):

$$D_1' = (G_0^d V_1 G_0^d)_m, \quad (\text{B.2})$$

which is

$$D(x_g, z_g, x_s, z_s, \omega) = \int_{-\infty}^{\infty} dx' \int_{-\infty}^{\infty} dz' \int_{-\infty}^{\infty} dx'' \int_{-\infty}^{\infty} dz'' \quad (\text{B.3})$$

$$\times G_0^d(x_g, z_g, x', z', \omega) V_1(x', z', x'', z'', \omega) G_0^d(x'', z'', x_s, z_s, \omega).$$

For the marine case, by first substituting the bilinear form of reference  $G_0^d$  (DeSanto, 1992)

$$G_0^d(x_g, z_g, x', z', \omega) = \int_{-\infty}^{\infty} dk'_x \int_{-\infty}^{\infty} dk'_z \frac{e^{ik'_x(x_g-x')} e^{ik'_z(z_g-z')}}{-k_x'^2 - k_z'^2 + k^2} \quad (\text{B.4})$$

and

$$G_0^d(x'', z'', x_s, z_s, \omega) = \int_{-\infty}^{\infty} dk''_x \int_{-\infty}^{\infty} dk''_z \frac{e^{ik''_x(x''-x_s)} e^{ik''_z(z''-z_s)}}{-k_x''^2 - k_z''^2 + k^2} \quad (\text{B.5})$$

into equation B.3, and then Fourier transforming on both sides of the resulting equation on  $x_g$  and  $x_s$ , the RHS becomes

$$RHS = \int_{-\infty}^{\infty} dx' \int_{-\infty}^{\infty} dz' \int_{-\infty}^{\infty} dx'' \int_{-\infty}^{\infty} dz'' \int_{-\infty}^{\infty} dx_g e^{-ik_g x_g} \int_{-\infty}^{\infty} dx_s e^{ik_s x_s} \quad (\text{B.6})$$

$$\times \int_{-\infty}^{\infty} dk'_x \int_{-\infty}^{\infty} dk'_z \frac{e^{ik'_x(x_g-x')} e^{ik'_z(z_g-z')}}{-k_x'^2 - k_z'^2 + k^2} V_1(x', z', x'', z'', \omega)$$

$$\times \int_{-\infty}^{\infty} dk''_x \int_{-\infty}^{\infty} dk''_z \frac{e^{ik''_x(x''-x_s)} e^{ik''_z(z''-z_s)}}{-k_x''^2 - k_z''^2 + k^2}.$$

Notice we use the convention mentioned on page R54 in Weglein *et al.* (2003), i.e.,

$$V_1(\mathbf{k}_1, -\mathbf{k}_2, \omega) = \int e^{-i\mathbf{k}_1 \cdot \mathbf{r}_1} V_1(\mathbf{r}_1, \mathbf{r}_2; \omega) e^{i\mathbf{k}_2 \cdot \mathbf{r}_2} d\mathbf{r}_1 d\mathbf{r}_2 \quad (\text{B.7})$$

where  $\mathbf{k}_1 \equiv (k_g, -q_g)$  and  $\mathbf{k}_2 \equiv (k_s, q_s)$ .

Combining the terms  $x_g$  and  $x_s$  in equation B.6, we have

$$\begin{aligned}
 RHS &= \int_{-\infty}^{\infty} dx' \int_{-\infty}^{\infty} dz' \int_{-\infty}^{\infty} dx'' \int_{-\infty}^{\infty} dz'' \int_{-\infty}^{\infty} dx_g e^{-i(k_g - k'_x)x_g} \int_{-\infty}^{\infty} dx_s e^{-i(k'_x - k_s)x_s} \quad (\text{B.8}) \\
 &\times \int_{-\infty}^{\infty} dk'_x \int_{-\infty}^{\infty} dk'_z \frac{e^{-ik'_x x'} e^{ik'_z(z_g - z')}}{-k'^2_x - k'^2_z + k^2} V_1(x', z', x'', z'', \omega) \int_{-\infty}^{\infty} dk''_x \int_{-\infty}^{\infty} dk''_z \frac{e^{ik''_x x''} e^{ik''_z(z'' - z_s)}}{-k''^2_x - k''^2_z + k^2} \\
 &= \int_{-\infty}^{\infty} dx' \int_{-\infty}^{\infty} dz' \int_{-\infty}^{\infty} dx'' \int_{-\infty}^{\infty} dz'' \delta(k'_x - k_g) \delta(k''_x - k_s) \\
 &\times \int_{-\infty}^{\infty} dk'_x \int_{-\infty}^{\infty} dk'_z \frac{e^{-ik'_x x'} e^{ik'_z(z_g - z')}}{-k'^2_x - k'^2_z + k^2} V_1(x', z', x'', z'', \omega) \int_{-\infty}^{\infty} dk''_x \int_{-\infty}^{\infty} dk''_z \frac{e^{ik''_x x''} e^{ik''_z(z'' - z_s)}}{-k''^2_x - k''^2_z + k^2} \\
 &= \int_{-\infty}^{\infty} dx' \int_{-\infty}^{\infty} dz' \int_{-\infty}^{\infty} dx'' \int_{-\infty}^{\infty} dz'' \\
 &\times \int_{-\infty}^{\infty} dk'_z \frac{e^{-ik_g x'} e^{ik'_z(z_g - z')}}{-k_g^2 - k'^2_z + k^2} V_1(x', z', x'', z'', \omega) \int_{-\infty}^{\infty} dk''_z \frac{e^{ik_s x''} e^{ik''_z(z'' - z_s)}}{-k_s^2 - k''^2_z + k^2}
 \end{aligned}$$

Introducing the definition:  $-k_g^2 + k^2 \equiv q_g^2$  and  $-k_s^2 + k^2 \equiv q_s^2$ , the *RHS* becomes,

$$\begin{aligned}
 RHS &= \int_{-\infty}^{\infty} dx' \int_{-\infty}^{\infty} dz' \int_{-\infty}^{\infty} dx'' \int_{-\infty}^{\infty} dz'' e^{-ik_g x'} e^{ik_s x''} \quad (\text{B.9}) \\
 &\times \int_{-\infty}^{\infty} dk'_z \frac{e^{ik'_z(z_g - z')}}{-k_g^2 - k'^2_z + k^2} V_1(x', z', x'', z'', \omega) \int_{-\infty}^{\infty} dk''_z \frac{e^{ik''_z(z'' - z_s)}}{-k_s^2 - k''^2_z + k^2} \\
 &= \int_{-\infty}^{\infty} dx' \int_{-\infty}^{\infty} dz' \int_{-\infty}^{\infty} dx'' \int_{-\infty}^{\infty} dz'' e^{-ik_g x'} e^{ik_s x''} \frac{e^{iq_g|z_g - z'|}}{2iq_g} V_1(x', z', x'', z'', \omega) \frac{e^{iq_s|z'' - z_s|}}{2iq_s},
 \end{aligned}$$

where, in the last step, we use (see e.g., DeSanto (1992))

$$\int_{-\infty}^{\infty} dk'_z \frac{e^{ik'_z(z_g - z')}}{-k_g^2 - k'^2_z + k^2} = \frac{e^{iq_g|z_g - z'|}}{2iq_g}, \quad (\text{B.10})$$

and similarly

$$\int_{-\infty}^{\infty} dk''_z \frac{e^{ik''_z(z'' - z_s)}}{-k_s^2 - k''^2_z + k^2} = \frac{e^{iq_s|z'' - z_s|}}{2iq_s}. \quad (\text{B.11})$$

Because the perturbation is below the measurement surface (*i.e.*,  $z' > z_g$  and  $z'' > z_s$ ), we can remove the absolute value as follows

$$\begin{aligned}
 RHS &= \int_{-\infty}^{\infty} dx' \int_{-\infty}^{\infty} dz' \int_{-\infty}^{\infty} dx'' \int_{-\infty}^{\infty} dz'' e^{-ik_g x'} e^{ik_s x''} \frac{e^{iq_g(z'-z_g)}}{iq_g} V_1(x', z', x'', z'', \omega) \frac{e^{iq_s(z''-z_s)}}{iq_s} \\
 &= \frac{e^{-iq_g z_g} e^{-iq_s z_s}}{iq_g iq_s} V_1(k_g, -q_g, k_s, q_s, \omega).
 \end{aligned} \tag{B.12}$$

Then, for the first-order term in type I, we have,

$$D(k_g, z_g, k_s, z_s, \omega) = \frac{e^{-iq_g z_g} e^{-iq_s z_s}}{2iq_g 2iq_s} V_1(k_g, -q_g, k_s, q_s, \omega). \tag{B.13}$$

• Equation (12') in Weglein *et al.* (2003) is

$$D'_2 = (G_0^d V_2 G_0^d)_m = -(G_0^d V_1 G_0^{fs} V_1 G_0^d)_m. \tag{B.14}$$

The *RHS* is

$$\begin{aligned}
 RHS &= - \int_{-\infty}^{\infty} dx' \int_{-\infty}^{\infty} dz' \int_{-\infty}^{\infty} dx'' \int_{-\infty}^{\infty} dz'' \int_{-\infty}^{\infty} dx''' \int_{-\infty}^{\infty} dz''' \int_{-\infty}^{\infty} dx'''' \int_{-\infty}^{\infty} dz'''' \\
 &\quad \times G_0^d(x_g, z_g, x', z', \omega) V_1(x', z', x'', z'', \omega) G_0^{fs}(x'', z'', x''', z''', \omega) \\
 &\quad \times V_1(x''', z''', x'''', z'''', \omega) G_0^d(x'''', z'''', x_s, z_s, \omega).
 \end{aligned} \tag{B.15}$$

Inserting the bilinear forms of  $G_0^d$  and  $G_0^{fs}$ ,

$$G_0^d(x_g, z_g, x', z', \omega) = \int_{-\infty}^{\infty} dk'_x \int_{-\infty}^{\infty} dk'_z \frac{e^{ik'_x(x_g-x')} e^{ik'_z(z_g-z')}}{-k_x'^2 - k_z'^2 + k^2}; \tag{B.16}$$

$$G_0^{fs}(x'', z'', x''', z''', \omega) = \int_{-\infty}^{\infty} dk_x'' \int_{-\infty}^{\infty} dk_z'' \frac{e^{ik_x''(x''-x''')} e^{ik_z''(z''+z''')}}{-k_x''^2 - k_z''^2 + k^2}; \quad (\text{B.17})$$

$$G_0^d(x'''' , z'''' , x_s, z_s, \omega) = \int_{-\infty}^{\infty} dk_x'''' \int_{-\infty}^{\infty} dk_z'''' \frac{e^{ik_x''''(x''''-x_s)} e^{ik_z''''(z''''-z_s)}}{-k_x''''^2 - k_z''''^2 + k^2}, \quad (\text{B.18})$$

into the above equation and Fourier transform on  $x_g$  and  $x_s$ , gives

$$\begin{aligned} RHS &= - \int_{-\infty}^{\infty} dx' \int_{-\infty}^{\infty} dz' \int_{-\infty}^{\infty} dx'' \int_{-\infty}^{\infty} dz'' \int_{-\infty}^{\infty} dx''' \int_{-\infty}^{\infty} dz''' \int_{-\infty}^{\infty} dx'''' \int_{-\infty}^{\infty} dz'''' \\ &\quad \times \int_{-\infty}^{\infty} dk_x' \int_{-\infty}^{\infty} dk_z' \frac{e^{ik_x'(x_g-x')} e^{ik_z'(z_g-z')}}{-k_x'^2 - k_z'^2 + k^2} V_1(x', z', x'', z'', \omega) \\ &\quad \times \int_{-\infty}^{\infty} dk_x'' \int_{-\infty}^{\infty} dk_z'' \frac{e^{ik_x''(x''-x''')} e^{ik_z''(z''+z''')}}{-k_x''^2 - k_z''^2 + k^2} V_1(x''', z''', x'''' , z'''' , \omega) \\ &\quad \times \int_{-\infty}^{\infty} dk_x'''' \int_{-\infty}^{\infty} dk_z'''' \frac{e^{ik_x''''(x''''-x_s)} e^{ik_z''''(z''''-z_s)}}{-k_x''''^2 - k_z''''^2 + k^2} \int_{-\infty}^{\infty} dx_g e^{-ik_g x_g} \int_{-\infty}^{\infty} dx_s e^{ik_s x_s} \\ &= - \int_{-\infty}^{\infty} dx' \int_{-\infty}^{\infty} dz' \int_{-\infty}^{\infty} dx'' \int_{-\infty}^{\infty} dz'' \int_{-\infty}^{\infty} dx''' \int_{-\infty}^{\infty} dz''' \int_{-\infty}^{\infty} dx'''' \int_{-\infty}^{\infty} dz'''' \\ &\quad \times \int_{-\infty}^{\infty} dk_z' \frac{e^{-ik_g x'} e^{ik_z'(z_g-z')}}{-k_g^2 - k_z'^2 + k^2} V_1(x', z', x'', z'', \omega) \int_{-\infty}^{\infty} dk_x'' \int_{-\infty}^{\infty} dk_z'' \frac{e^{ik_x''(x''-x''')} e^{ik_z''(z''+z''')}}{-k_x''^2 - k_z''^2 + k^2} \\ &\quad \times V_1(x''', z''', x'''' , z'''' , \omega) \int_{-\infty}^{\infty} dk_z'''' \frac{e^{ik_s x''''} e^{ik_z''''(z''''-z_s)}}{-k_s^2 - k_z''''^2 + k^2} \\ &= - \int_{-\infty}^{\infty} dx' \int_{-\infty}^{\infty} dz' \int_{-\infty}^{\infty} dx'' \int_{-\infty}^{\infty} dz'' \int_{-\infty}^{\infty} dx''' \int_{-\infty}^{\infty} dz''' \int_{-\infty}^{\infty} dx'''' \int_{-\infty}^{\infty} dz'''' \\ &\quad \times e^{-ik_g x'} \int_{-\infty}^{\infty} dk_z' \frac{e^{ik_z'(z_g-z')}}{-k_g^2 - k_z'^2 + k^2} V_1(x', z', x'', z'', \omega) \int_{-\infty}^{\infty} dk_x'' \int_{-\infty}^{\infty} dk_z'' \frac{e^{ik_x''(x''-x''')} e^{ik_z''(z''+z''')}}{-k_x''^2 - k_z''^2 + k^2} \\ &\quad \times V_1(x''', z''', x'''' , z'''' , \omega) e^{ik_s x''''} \int_{-\infty}^{\infty} dk_z'''' \frac{e^{ik_z''''(z''''-z_s)}}{-k_s^2 - k_z''''^2 + k^2} \end{aligned} \quad (\text{B.19})$$

Recalling the definitions of  $-k_g^2 + k^2 = q_g^2$  and  $-k_s^2 + k^2 = q_s^2$ , we have

$$\begin{aligned}
 RHS &= - \int_{-\infty}^{\infty} dx' \int_{-\infty}^{\infty} dz' \int_{-\infty}^{\infty} dx'' \int_{-\infty}^{\infty} dz'' \int_{-\infty}^{\infty} dx''' \int_{-\infty}^{\infty} dz''' \int_{-\infty}^{\infty} dx'''' \int_{-\infty}^{\infty} dz'''' \\
 &\quad \times e^{-ik_g x'} \frac{e^{iq_g |z_g - z'|}}{2ig_g} V_1(x', z', x'', z'', \omega) \int_{-\infty}^{\infty} dk_x'' \int_{-\infty}^{\infty} dk_z'' \frac{e^{ik_x''(x'' - x''')} e^{ik_z''(z'' + z''')}}{-k_x''^2 - k_z''^2 + k^2} \\
 &\quad \times V_1(x''', z''', x'''', z'''', \omega) e^{ik_s x''''} \frac{e^{iq_s |z'''' - z_s|}}{2ig_s} \\
 &= - \int_{-\infty}^{\infty} dx' \int_{-\infty}^{\infty} dz' \int_{-\infty}^{\infty} dx'' \int_{-\infty}^{\infty} dz'' \int_{-\infty}^{\infty} dx''' \int_{-\infty}^{\infty} dz''' \int_{-\infty}^{\infty} dx'''' \int_{-\infty}^{\infty} dz'''' \\
 &\quad \times e^{-ik_g x'} \frac{e^{iq_g(z' - z_g)}}{2ig_g} V_1(x', z', x'', z'', \omega) \int_{-\infty}^{\infty} dk_x'' \int_{-\infty}^{\infty} dk_z'' \frac{e^{ik_x''(x'' - x''')} e^{ik_z''(z'' + z''')}}{-k_x''^2 - k_z''^2 + k^2} \\
 &\quad \times V_1(x''', z''', x'''', z'''', \omega) e^{ik_s x''''} \frac{e^{iq_s(z'''' - z_s)}}{2ig_s}
 \end{aligned} \tag{B.20}$$

Considering the integral on  $x', z', x''', z''''$  and  $x'', x'''$  as a Fourier transform based on the convention (equation B.7), we have

$$\begin{aligned}
 RHS &= - \int_{-\infty}^{\infty} dx'' \int_{-\infty}^{\infty} dz'' \int_{-\infty}^{\infty} dx''' \int_{-\infty}^{\infty} dz''' \frac{e^{-iq_g z_g}}{2ig_g} V_1(k_g, -q_g, x'', z'', \omega) \\
 &\quad \times \int_{-\infty}^{\infty} dk_x'' \int_{-\infty}^{\infty} dk_z'' \frac{e^{ik_x''(x'' - x''')} e^{ik_z''(z'' + z''')}}{-k_x''^2 - k_z''^2 + k^2} V_1(x''', z''', k_s, q_s, \omega) \frac{e^{-iq_s z_s}}{2ig_s} \\
 &= - \int_{-\infty}^{\infty} dz'' \int_{-\infty}^{\infty} dz''' \frac{e^{-iq_g z_g}}{2ig_g} V_1(k_g, -q_g, k_x'', z'', \omega) \\
 &\quad \times \int_{-\infty}^{\infty} dk_x'' \int_{-\infty}^{\infty} dk_z'' \frac{e^{ik_z''(z'' + z''')}}{-k_x''^2 - k_z''^2 + k^2} V_1(k_x'', z''', k_s, q_s, \omega) \frac{e^{-iq_s z_s}}{2ig_s}
 \end{aligned} \tag{B.21}$$

Similarly, defining  $-k_x''^2 + k^2 \equiv q_x''^2$ , we have

$$\begin{aligned}
 RHS &= - \int_{-\infty}^{\infty} dz'' \int_{-\infty}^{\infty} dz''' \frac{e^{-iq_g z_g}}{2ig_g} V_1(k_g, -q_g, k_x'', z'', \omega) \\
 &\quad \times \int_{-\infty}^{\infty} dk_x'' \frac{e^{iq_x''|z''+z'''}|}{-2ig_x''} V_1(k_x'', z''', k_s, q_s, \omega) \frac{e^{-iq_s z_s}}{2ig_s} \\
 &= - \int_{-\infty}^{\infty} dz'' \int_{-\infty}^{\infty} dz''' \frac{e^{-iq_g z_g}}{2ig_g} V_1(k_g, -q_g, k_x'', z'', \omega) \\
 &\quad \times \int_{-\infty}^{\infty} dk_x'' \frac{e^{iq_x''(z''+z''')}}{2ig_x''} V_1(k_x'', z''', k_s, q_s, \omega) \frac{e^{-iq_s z_s}}{2ig_s} \\
 &= - \frac{e^{-iq_g z_g}}{2ig_g} V_1(k_g, -q_g, k_x'', q_x'', \omega) \int_{-\infty}^{\infty} dk_x'' \frac{1}{2ig_x''} V_1(k_x'', -q_x'', k_s, q_s, \omega) \frac{e^{-iq_s z_s}}{2ig_s} \\
 &= - \frac{e^{-iq_g z_g}}{2ig_g} \frac{e^{-iq_s z_s}}{2ig_s} \int_{-\infty}^{\infty} dk V_1(k_g, -q_g, k, q, \omega) \frac{1}{2ig} V_1(k, -q, k_s, q_s, \omega)
 \end{aligned} \tag{B.22}$$

Notice that the + sign in  $\frac{e^{iq_x''|z''+z'''}|}{-2ig_x''}$  enables us to remove the absolute value.

The *LHS* of equation B.14 is

$$LHS = \frac{e^{-iq_g z_g}}{2iq_g} \frac{e^{-iq_s z_s}}{2iq_s} V_2(k_g, -q_g, k_s, q_s, \omega) \tag{B.23}$$

Comparing equation B.23 and equation B.22, we have

$$V_2(k_g, -q_g, k_s, q_s, \omega) = - \int_{-\infty}^{\infty} dk V_1(k_g, -q_g, k, q, \omega) \frac{1}{2ig} V_1(k, -q, k_s, q_s, \omega) \tag{B.24}$$

- Equation (13') in Weglein *et al.* (2003)

$$\begin{aligned}
 D'_3 &= - (G_0^d V_1 G_0^{fs} V_1 G_0^{fs} V_1 G_0^d)_m & (B.25) \\
 &\quad - (G_0^d V_1 G_0^{fs} V_2 G_0^d)_m \\
 &\quad - (G_0^d V_2 G_0^{fs} V_1 G_0^d)_m \\
 &= + (G_0^d V_1 G_0^{fs} V_1 G_0^{fs} V_1 G_0^d)_m
 \end{aligned}$$

Following the procedures from equation B.14 through equation B.22, the first term in B.25 becomes

$$- \int_{-\infty}^{\infty} dk V_1(k_g, -q_g, k, q, \omega) \frac{1}{2ig} \int_{-\infty}^{\infty} dk' V_1(k, -q, k', q', \omega) \frac{1}{2ig'} V_1(k', -q', k_s, q_s, \omega) \quad (B.26)$$

and the second term becomes

$$- \int_{-\infty}^{\infty} dk V_1(k_g, -q_g, k, q, \omega) \frac{1}{2ig} V_2(k, -q, k_s, q_s, \omega) \quad (B.27)$$

Substituting  $V_2(k_g, -q_g, k, q, \omega)$  (equation B.24) into equation B.27, we have

$$\int_{-\infty}^{\infty} dk V_1(k_g, -q_g, k, q, \omega) \frac{1}{2ig} \int_{-\infty}^{\infty} dk' V_1(k, -q, k', q', \omega) \frac{1}{2ig'} V_1(k', -q', k_s, q_s, \omega) \quad (B.28)$$

Therefore, equation B.28 cancels out equation B.26, and a reduction occurs.

- Type II terms

- Equation (11'') in Weglein *et al.* (2003) is

$$D' = (G_0^d V_1' G_0^d)_m, \quad (B.29)$$

which is

$$D'(k_g, z_g, k_s, z_s, \omega) = \frac{e^{-iq_g z_g}}{2iq_g} \frac{e^{-iq_s z_s}}{2iq_s} V_1'(k_g, -q_g, k_s, q_s, \omega). \quad (\text{B.30})$$

Notice the *LHS* of equation B.30 and B.13 are different:  $D_1'$  is data with the free-surface multiples and  $D'$  is data without free-surface multiples.

- Equation (12'') in Weglein *et al.* (2003) is

$$(G_0^d V_2' G_0^d)_m = -(G_0^d V_1' G_0^d V_1' G_0^d)_m. \quad (\text{B.31})$$

We derive the *RHS* of equation B.31 following the same procedure as we derive the *RHS* of equation B.14. The difference resides the middle reference Green's function. With the middle reference Green's function being  $G_0^d$ , instead of  $G_0^{fs}$ , we cannot lift the absolute value in equation B.22 without specifying the relationship between  $z'$  and  $z''$ . In other words, without specifying the relationship between  $z'$  and  $z''$ , the *RHS* of equation B.31 is not computable from our data on the measurement surface. Hence, each type II term is different and not reducible. The same argument explains the differences in higher-order terms in type II.

